Design of Experiment Based Optimization of an in Vitro Direct Contact Triculture Blood Brain Barrier Model for Permeability Screening

Kelsey E Lubin
Purdue University College of Pharmacy
Gregory T. Knipp (gknipp@purdue.edu)
Department of Industrial and Physical Pharmacy, Purdue University, 575 Stadium Mall Drive, West Lafayette, Indiana 47907, USA. https://orcid.org/0000-0002-4199-2929

Research

Keywords: Blood brain barrier, permeability, design of experiments, optimization, astrocytes, pericytes, brain microvessel endothelium, triculture, direct cell-cell contact

Posted Date: June 10th, 2021

DOI: https://doi.org/10.21203/rs.3.rs-592200/v1

DESIGN OF EXPERIMENT BASED OPTIMIZATION OF AN *IN VITRO* DIRECT CONTACT TRICULTURE BLOOD BRAIN BARRIER MODEL FOR PERMEABILITY SCREENING

Kelsey E. Lubin and Gregory T. Knipp*

* Corresponding author

Department of Industrial and Physical Pharmacy, Purdue University, 575 Stadium Mall Drive, West Lafayette, Indiana 47907, USA.

Running Title: DOE Optimization of a Direct Contact Triculture BBB Model

Submitted to: Fluids and Barriers of the CNS

* Corresponding author to whom correspondence should be addressed:
Gregory T. Knipp, Ph.D.
Industrial and Physical Pharmacy
College of Pharmacy
Purdue University
575 Stadium Mall Drive
West Lafayette, IN 47907-2091
Telephone: 765-494-3765
Fax: 765-494-6545
E-mail: gknipp@purdue.edu

Abstract

Background: The *in vivo* restrictive properties of the blood brain barrier (BBB) largely arise from astrocyte and pericyte synergistic cell signaling interactions that underlie the brain microvessel endothelial cells (BMEC). *In vivo* relevant direct contact between astrocytes, pericytes, and BMECS, to our knowledge, has not been established in conventional Transwell® based *in vitro* screening models of the BBB. We hypothesize that a design of experiments (DOE) optimized direct contact layered triculture model will offer more *in vivo* relevance for screening in comparison to indirect models.

Methods: Plating conditions including the seeding density of all three cell types, matrix protein, and culture time were assessed in DOE_P. DOE_P was followed by DOE_{M1} and DOE_{M2} to assess the influence of medium additives on barrier properties. The permeability of 4 kD dextran, a paracellular marker, was the measured response to arrive at the optimal plating conditions. The optimized model was further assessed for p-glycoprotein function using a substrate and inhibitor along with a set of BBB paracellular and transcellular markers at varying permeation rates.

Results: DOE_P revealed that length of culture post endothelial cell plating correlated highest with paracellular tightness. In addition, seeding density of the endothelial cell layer influenced paracellular tightness at earlier times of culture, and its impact decreased as culture is extended. Medium additives had varying effects on barrier properties as seen from DOE_{M1} and DOE_{M2}. At optimal conditions, the model revealed P-gp function along with the ability to differentiate between BBB positive and negative permeants.

Conclusions: We have demonstrated that the implementation of DOE based optimization for biologically based systems is an expedited method to establish multi-component *in vitro* cell

models. The direct contact BBB triculture model reveals that the physiologically relevant layering of the three cell types is a practical method of culture to establish a screening model compared to indirect plating methods that incorporate physical barriers between cell types. Additionally, the ability of the model to differentiate between BBB positive and negative permeants suggests that this model may be an enhanced screening tool for potential neuroactive compounds.

Keywords: Blood brain barrier, permeability, design of experiments, optimization, astrocytes, pericytes, brain microvessel endothelium, triculture, direct cell-cell contact

Background

There is a continuing need for screening models that will facilitate the development of therapeutic agents aimed at mitigating brain disorders, particularly as there is a rapidly increasing prevalence of neurodegenerative and neurodevelopmental diseases.(1) The costs associated with developing neurotherapeutics is significant in large part due to the high rates of attrition in later stages of development.(2) The implementation of a low cost, predictive, and physiologically relevant *in vitro* screening model to more rigorously facilitate hit to lead candidate selection providing greater *in vivo* correlative rank ordering of potential compounds or drug delivery systems for further development is imperative.

Many have theorized that the high rates of attrition are predominantly due to the inability of drug candidates to cross the blood brain barrier (BBB).(1–3) The BBB has traditionally been viewed as the brain microvessel endothelial cells (BMECs) that line the capillaries of the brain to maintain a homeostatic environment. The BBB separates the brain parenchyma from the systemic circulation and prevents permeation of potential xenobiotics into the brain interstitial

fluids.(4,5) The BBB endothelium is unique in comparison to the periphery due to the high expression of efflux proteins, drug transporters, metabolizing enzymes, and the presence of restrictive tight junctions.(6,7) Tight junctions in the brain are formed between adjacent BMECs by a complex of transmembrane intracellular cleft spanning proteins such as the occludins and claudins 3 and 5, which anchor to cytosolic scaffolding proteins supported by the actin cytoskeleton.(8–10) The presence of restrictive tight junctions limits the permeation of small hydrophilic compounds, forcing compounds to move transcellularly in order to cross the BBB.

The high expression levels of non-substrate specific ATP-binding cassette (ABC) transporters such as P-glycoprotein (P-gp) and Breast Cancer Resistance Protein (BCRP) results in a high degree of efflux for molecules that attempt to cross the BBB through the transcellular pathway.(11) The presence of efflux transporters may limit the permeation of potential neurotoxicants, while also presenting a challenge for drug delivery as a number of intended neurotherapeutics tend to be lipophilic, favoring multidrug-resistant isoform efflux.(12) Due to their unique presence in the BBB, restrictive tight junctions and functional efflux proteins are key validation characteristics when establishing an *in vitro* BBB screening model.

The *in vivo* BBB phenotype is also largely modulated by the presence of supporting cellular and non-cellular components including astrocytes, pericytes, neurons, and the basal lamina. Together, these components make up the neurovascular unit (NVU), which are each essential for the function of the BBB *in vivo*. Astrocytes are a glial cell type that fully surround the endothelium and are linked to each other via gap junctions.(13) Single astrocytes have been shown to interact with up to four different neurons and five blood vessels, making them the cellular link between the endothelium and brain parenchyma.(14–16) Astrocytes participate in ion and water regulation due to the localization of aquaporin 4 and ion channels in the astrocytic

end-feet and have been linked to the secretion of basal lamina proteins.(10,17) Additionally, astrocytes influence BMEC growth, modulation through extracellular signaling, play an important metabolic role, and assist in the functional maintenance through the secretion of soluble factors which have been shown to be essential for NVU homeostasis.(18–21) Towards the latter point, several *in vitro* and *in vivo* studies have demonstrated that changes in BBB integrity may result from a deficiency of certain astrocytic soluble factors.(18–21)

Pericytes are found enveloped in the basal lamina of the NVU between the astrocytes and endothelium. However, pericyte distribution is not continuous and in general cover approximately one third of the BMEC basal layer, with higher densities observed regiospecifically within the brain.(22) Pericytes are believed to play a similar role as astrocytes in NVU modulation through the secretion of soluble factors, but are unique in their role in NVU formation and maintenance, specifically during development.(23,24) Pericyte-endothelial crosstalk occurs through a number of signal cascades including platelet-derived growth factor B (PDGF-B) and transforming growth factor-β (TGF-β), as well as others.(25) Interactions between the pericytes and endothelium occurs within the basal lamina due to the relative location of embedded pericytes in the shared basement membrane, potentially suggesting that the composition of the extracellular matrix plays a role in BBB development and maintenance. The basal lamina is a non-cellular component of the NVU and is responsible for maintaining integrity of the BBB by anchoring the cellular components. There are a significant number of basement membrane proteins that include fibronectin, collagen IV, laminins, and vitronectin that form the matrix which is approximately 20 nm thick *in vivo*.(6,26,27) Given the multiple components that make up the NVU, cellular and non-cellular, we propose that the BBB should be viewed as the

directly interacting BMECs, pericytes and astrocytes of the NVU as a whole rather than simply the contributions of the BMECs.

Since its establishment in 2005, the hTERT oncogene and SV40 immortalized human cerebral microvessel endothelial cell line (hCMEC/D3) developed from primary endothelial cells of an epilepsy patient has been the most widely used immortalized endothelial cell line for BBB *in vitro* models.(28,29) Although it is widely used, studies (as well as our observations, unpublished results) have revealed that hCMEC/D3 cells can have relatively "leaky" tight junctions and demonstrate a functional reduction in efflux transporter expression with passaging.(30–33) An alternative immortalized human brain endothelium is the HBEC-5i cell line that was singly transfected with SV40 and originates from a patient pool of cerebral cortex fragments, lacking pathological abnormalities.(34,35) The HBEC-5i has been used predominantly in the study of cerebral malaria; however, these studies have established the potential for this cell line to be used for BBB *in vitro* permeability screening.(35–38) These cells have been observed to express a high number of electron-dense tight junctions as seen under electron scanning microscopy, as well as provide high transendothelial electrical resistance (TEER) and low permeability comparable to other immortalized BMECs.(35) Recently, the HBEC-5i cell line has been used for *in vitro* modeling of the BBB showing functional expression of ABC transporters and stable barrier properties over multiple days of culture, suggesting they are a viable alternative to the hCMEC/D3 cell line and other immortalized BMEC sources.(39,40)

Given the interaction of multiple cell types that maintain the BBB phenotype in the NVU, many *in vitro* models include astrocytes and pericytes in conjunction with BMECs.(30,41–45) Typically, these models involve seeding the endothelium on the apical surface of the filter and

the supporting astrocytes and pericytes in the basolateral chamber or on the reverse side of the filter.(46–50) In this study we have further developed and optimized our previously established direct contact, layered coculture model to form a triculture system with the inclusion of pericytes to further increase the physiological relevance of the *in vitro* model.(51) The direct contact, layered triculture model is cultured by seeding astrocytes, followed by pericytes, then the endothelium all on the apical side of a filter support to reflect the *in vivo* configuration and cell-cell contacts of the BBB in the *in vivo* NVU (Fig. 1). In our previous studies, we have utilized a One Factor at a Time approach to optimize culturing variables in a laborious and time-consuming manner. Given the multiple factors that influence the performance of this model, we have now utilized a design of experiments (DOE) approach to determine optimal culturing conditions by assessing the influence of multiple variables on barrier properties in a single experiment. This study has demonstrated that a DOE based approach, typically utilized in non-biological process optimization, can be used to optimize other multi-factor cell-based *in vitro* systems by assessing variable influence on model performance. Additionally, the results of this study demonstrate the importance of direct cell contact in *in vitro* models and suggests that increasing physiological relevance of *in vitro* models to mimic the *in vivo* NVU BBB can further enhance screening tools for neurotherapeutic development.

Methods

Materials

Transwell® filters of 12 mm 0.4 µm pore size, T-75 culture flasks, Matrigel®, mouse laminin, and type I rat tail collagen were purchased from Corning (Corning, NY, USA). Hank's balanced salt solution (HBSS) and Dulbecco's Modified Eagle Medium/Nutrient Mixture F-12 (DMEM/F-12) were obtained from Gibco (Carlsbad, CA, USA). Fetal bovine serum (FBS),

hydrocortisone, lithium chloride, retinoic acid, rhodamine 123 (R123), elacridar, digoxin, carbamazepine, colchicine, clozapine, caffeine, and prazosin hydrochloride were purchased from MilliporeSigma (St. Louis, MO, USA). HEPES (2-[4-(2-hydroxyethyl)piperazin-1-yl]-ethanesulfonic acid) and calcium chloride dihydrate were obtained from J.T. Baker (Phillipsburg, NJ, USA). Dexamethasone was obtained from MP Biomedicals (Santa Ana, CA, USA). Endothelial cell growth supplement (ECGS) was purchased from Alfa Aesar (Haverhill, MA, USA). Fluorescein isothiocyanate (FITC) labeled 4 kD dextran was purchased from Chondrex (Redmond, WA, USA). Poly-L-lysine (PLL) was purchased from Trevigen (Gaithersburg, MD, USA). Radiolabeled compounds [14C]-mannitol, -sucrose, -inulin, -PEG-4000, and [3H]-L-histidine were purchased from Moravek Biochemicals Inc. (Brea, CA, USA). Human astrocytes, human brain vascular pericytes, astrocyte medium, pericyte medium, and astrocyte and pericyte growth factors were all obtained from ScienCell Research Laboratories (Carlsbad CA, USA). HBEC-5i cells were purchased from ATCC (Manassas, VA, USA).

Cell Culture

Human Brain Endothelial Cells (HBEC-5i) were maintained in T-75 culture flasks pre-coated with Type I rat tail collagen with medium changes every 3 days and culturing at 80-90% confluency. The cells were utilized in the studies between passages 22 and 30. HBEC-5i culture medium was made up of Dulbecco's Modified Eagle Medium/Nutrient Mixture F-12 (DMEM/F-12) supplemented with 10% FBS, 15 mM HEPES, and 40 ug/mL endothelial cell growth supplement (ECGS). Human astrocytes and human brain vascular pericytes are maintained in T-75 culture flasks pre-coated with poly-L-lysine with medium changes every 3 days and subculturing at 80-90% confluency. For the studies presented herein, the astrocytes and pericytes were utilized between passage 4 and 10. Astrocyte culture medium was made up of Astrocyte

Medium supplemented with 5% FBS, astrocyte growth supplement, and penicillin/streptomycin. Pericyte culture medium was made up of Pericyte Medium supplemented with 5% FBS, pericyte growth supplement, and penicillin/streptomycin.

Experimental Design for Optimization

Optimization of plating conditions (cell seeding densities, extracellular matrix protein, and length of culture) and medium additives were performed in sequential design of experiment (DOE) analyses. For plating studies JMP® 13.2 from SAS statistical software was used to determine the plating conditions of each experimental run for a total of 39 combinations by utilizing a 5 factor, 2 level, custom design (DOE_P). Each run was done in a single replicate with DOE_P selected conditions to determine best levels for each variable and then the combined optimized conditions were further confirmed in subsequent experiments in triplicate. Table 1 lists the various factors and the respective levels of each.

Table 1. Plating factors and conditions for DOE (DOE_P)

Factor	Selected Range*
Astrocyte Seeding Density	20,000 – 60,000 cells/cm^2
Pericyte Seeding Density	20,000 – 60,000 cells/cm^2
HBEC-5i Seeding Density	50,000 – 110,000 cells/cm^2
Study Day	Day 5 – 9
Extracellular Matrix	Collagen I, Matrigel, Laminin

* 3 levels each factor

Similarly, medium optimization was performed in two analyses using a custom design DOE to determine medium conditions that resulted in the tightest barrier properties. The first analysis (DOE_{M1}) was performed using HEPES, hydrocortisone, dexamethasone, LiCl, calcium, and retinoic acid, using the selected date for permeability analysis at 9 days post endothelial cell plating (Table 2). A second analysis (DOE_{M2}) was performed, based on the results of the first,

using hydrocortisone, dexamethasone, LiCl, and retinoic acid at both 5 and 7 days post endothelial cell plating (Table 3).

Table 2. Medium optimization with evaluation on Day 9 (DOE_{M1})

Factor	Selected Range*
HEPES	15 – 25 mM
Hydrocortisone	0 – 1.4 µM
Dexamethasone	0 – 10 µM
Lithium Chloride	0 – 10 mM
Calcium	0 – 1 mM
Retinoic Acid	0 – 10 µM
Study Day	Day 9

* 2 levels each factor (presence or absence of given additive)

Table 3. Medium optimization with evaluation on Day 5 and 7 (DOE_{M2})

Factor+	Selected Range*
Hydrocortisone	0 – 1.4 µM
Dexamethasone	0 – 10 µM
Lithium Chloride	0 – 10 mM
Retinoic Acid	0 – 10 µM
Study Day	Day 5 or 7

+All medium supplemented with 15 mM HEPES

* 2 levels each factor (presence or absence of given additive)

Plating Direct Contact Triculture on Transwell® Filter Support

For the DOE_P studies, filters were pre-coated with poly-L-lysine (PLL) by pre-coating 12 mm, 0.4 µm pore Transwell® inserts with 5 µg/cm^2 PLL. Astrocytes were plated at seeding densities of 20,000, 40,000, or 60,000 cells/cm^2 and allowed to grow for 48 hours. After 48 hours of astrocyte growth, astrocyte medium was removed and pericytes were seeded atop the astrocyte lawn at seeding densities of 20,000, 40,000, or 60,000 cells/cm^2 and allowed to grow for 48 hours. After 48 hours of pericyte growth, apical medium was replaced with the specified ECM protein solution. Astrocyte-pericyte lawn filters were coated with one of the following ECM proteins at the respective concentrations: Matrigel® 25 µL/cm^2 (2.5 µg/cm^2), Laminin 5 µg/cm^2,

208 or Type I Rat Tail Collagen 5 μg/cm^2. To coat inserts, Matrigel®, Laminin, or collagen I aliquots
209 were diluted in HBSS with Ca^{2+} and Mg^{2+} and 0.5 mL dispensed onto to each respective 12 mm
210 insert and left to incubate with the respective ECM protein for 45 min at 37 °C. After incubation,
211 the ECM solution was removed and HBEC-5i cells were plated at seeding densities of 50,000,
212 80,000, or 110,000 cells/cm^2 and allowed to grow for 5, 7, or 9 days prior to permeability
213 measurements. Cultures were maintained in complete HBEC-5i medium with medium changes
214 every other day following endothelial cell plating. Transendothelial electrical resistance (TEER)
215 was measured every 24 hours after HBEC-5i plating using a 4 mm Chopstick electrode with
216 EVOM2 Volt/Ohm Meter (World Preclinical Instruments), and normalized based on resistance
217 across blank filter supports.

218 In $DOE_{M1/2}$ studies, the culturing methodology described above was used with the
219 modification that the complete HBEC-5i culture medium was supplemented with the DOE
220 selected factors and introduced to cultures 24 hours post endothelial plating with medium
221 changes every other day until the day of study. Medium for $DOE_{M1/2}$ was prepared from
222 concentrated stock solutions of 1 M HEPES in water, 4.6 mM hydrocortisone in ethanol, 3.8 mM
223 dexamethasone in DMSO, 11.8 M LiCl in water, 1.7 M $CaCl_2$ in water, and 33.3 mM retinoic
224 acid in DMSO. Final solvent content was normalized across all runs to eliminate solvent effect as
225 a confounding factor in the study.

226 **Plating Monoculture and Direct Contact Coculture on Transwell® Filter Support**

227 Monoculture (HBEC-5i alone) and direct contact coculture (astrocyte-HBEC-5i and
228 pericyte-HBEC-5i) models were used for comparison with the DOE optimized direct contact
229 triculture. For monoculture studies, 12 mm, 0.4 μm pore Transwell® inserts were pre-coated with
230 25 μL/cm^2 Matrigel®. HBEC-5i cells were plated on Matrigel® coated filters at a density of

80,000 cells/cm^2 and cultured for 9 days with medium changed every other day. Direct contact cocultures were plated according to methods developed by Kulczar *et al.* with some modifications.(51) Transwell® filters were pre-coated with 5 µg/cm^2 PLL followed by seeding of astrocytes or pericytes at 20,000 cells/cm^2 and allowed to grow for 48 hours. At 48 hours post astrocyte or pericyte plating, HBEC-5i cells at 80,000 cells/cm^2 were seeded directly atop the lawn of pre-seeded cells and cultured for an additional 9 days with medium changed every other day.

Permeability Assays

To optimize conditions, permeability was measured using 4 kD FITC-dextran at an initial concentration of 0.25 mg/mL in HBSS with Ca^{2+} and Mg^{2+}. Triculture DOE generated plating conditions and the optimized parameters were washed and left to equilibrate in HBSS at 37 °C for 30 minutes prior to the start of the permeability assay. Permeability was performed at 37 °C on a rocking platform maintaining sink conditions and sampling at 15, 30, 45, 60, and 90 minutes. Samples of 100 µL from each basolateral chamber were removed at each time point and placed into a 96-well black flat-bottomed well plate for fluorescence reading. After sampling, naïve HBSS was added back to the basolateral chamber to maintain hydrostatic pressure and the lost mass was accounted for in the calculated permeation rates. Samples were analyzed using a BioTek Synergy 4 plate reader at excitation of 485 nm and emission of 530 nm. Apparent permeability (P_{app}) was calculated using equation 1 (eq. 1)

$$P_{app} = \frac{dM/dT}{C_0 \times A} \quad \text{(eq. 1)}$$

where dM/dT is the amount of Dextran that moves across the filter over time, Co is the initial concentration in the donor (apical) chamber, and A is the surface area of the filter support. The

effective permeability (P_{eff}, permeability contributions of cell layer alone) of each condition was determined using equation 2 (eq. 2) where the P_{filter} value used is that of the ECM used in the given condition.

$$\frac{1}{P_{app}} = \frac{1}{P_{eff}} + \frac{1}{P_{filter}} \quad \text{(eq. 2)}$$

Apparent permeability of additional paracellular markers of varying sizes ([^{14}C]-mannitol, [^{14}C]-sucrose, [^{14}C]-inulin, and [^{14}C]-PEG-4000) was determined in the optimized direct contact triculture. Permeability assays were performed as stated above with an initial concentration of 0.25 µCi/mL in HBSS for all markers and analysis performed utizing a liquid scintillation counter.

A range of BBB positive and negative permeants were used to further evaluate barrier properties of the optimized model. The permeability of [^{3}H]-L-histidine, carbamazepine, colchicine, digoxin, clozapine, and prazosin was determined by preparing 10 mM stock solutions of each compound in DMSO, with the exception of [^{3}H]-L-histidine. For each study, the final concentration of DMSO was equivalent at 1% (v/v). Permeability of [^{3}H]-L-histidine was determined using the same method as stated above for radiolabeled paracellular markers. Working solutions of non-radiolabeled compounds were prepared at a concentration of 25 µM in HBSS with permeability measurements performed as stated above and sampling at 30, 60, 90, 120, and 150 minutes. Analysis for these compounds was performed using high performance liquid chromatography (HPLC). Permeability was calculated according to equation 1.

The function of P-gp in the triculture model was determined using P-gp substrate rhodamine 123 (R123) in the presence and absence of the inhibitor elacridar. Stock solutions of

277 R123 (2 mM) and elacridar (10 mM) were prepared in DMSO. Working solutions of 10 µM
278 R123 and 2 µM elacridar were prepared in HBSS with 1% DMSO. For inhibition studies,
279 tricultures plated on permeable filter supports were pre-incubated with 2 µM elacridar for 45
280 minutes prior to the addition of R123. Samples were removed at 30, 60, 90, and 120 minutes and
281 analysis was performed using the BioTek Synergy 4 plate reader at excitation of 485 nm and
282 emission of 530 nm. Permeability was calculated according to equation 1.

283 **High Performance Liquid Chromatography**

284 Analysis of carbamazepine, caffeine, colchicine, digoxin, clozapine, and prazosin was
285 performed on an Agilent 1100 reverse phase HPLC with variable wavelength detection (VWD),
286 as briefly described below and summarized in Table 4.

287 **Table 4.** High Performance Liquid Chromatography analyses performed on an Agilent 1100
288 reverse phase HPLC with variable wavelength detection (VWD).

Compound	Column temperature	Mobile phase (water:acetonitrile)	Flow rate (mL/min)	Absorbance measurement (nm)
Caffeine	ambient	90:10	1.0	275
Carbamazepine	40 °C	65:35	1.5	284
Clozapine	40 °C	45:55	1.5	254
Colchicine	40 °C	75:25	1.5	354
Digoxin	40 °C	70:30	1.1	218
Prazosin	40 °C	65:35	1.5	254

All samples were run isochratically through an Ascentis® C-18 15 x 4.6 mm, 5 µm column, at 25 µL injection volume, using water and acetonitrile (ACN) for all mobile phase.

289 **Statistical Analysis**

290 Custom experimental designs based on categorical and discrete continuous factors were
291 generated by JMP 13.2 statistical software. Analysis of each DOE was done by fitting models
292 based on the P_{eff} of 4 kD dextran response to standard least squares to determine optimal
293 conditions. In comparison studies, all conditions were performed in triplicate (n=3) and subjected
294 to Student's *t*-test or one-way ANOVA with Tukey Kramer post-hoc test. A p-value of 0.05 was
295 considered to be statistically significant.

Results

Plating Optimization (DOE_P)

Traditionally, a One-Factor-at-a-Time (OFAT) approach is used to assess the impact of variable changes in cell-based models and processes, where one variable (e.g., cell density) is optimized in the presence of several other unoptimized variables that results in an inefficient and laborious manner. A Design of Experiments (DOE) based approach allows for the influence of multiple factors to be observed on a measured response to arrive at an optimal level for each given variable. Furthermore, it allows one to more rapidly identify optimized growth conditions in a time and labor efficient manner. Our previous studies towards establishing a direct contact triculture (unpublished results) and our direct contact coculture model, were used to inform our selection of respective seeding densities for all three cell types, ECM used to aid endothelial attachment, and length of culture of the endothelium that consisted of the initial selected factor ranges.(51) Optimal plating conditions were determined using P_{eff} values to account for the differences associated with ECM coatings. Conditions 8 (60 HA, 60 HBVP, 110 EC, Laminin, Day 9) and 20 (20 HA, 20 HBVP, 110 EC, Laminin, Day 9) exhibited the lowest Peff values at 3.2×10^{-6} cm/sec (Fig. 2). Condition details and tabulated P_{eff} data of DOE_P are noted in Additional File 1.

Based on the data trends, the culture length between the assay day was determined to have the largest impact on paracellular permeability resulting in significantly lower 4 kD dextran permeability at day 9 compared to days 5 and 7. When separating the data by study day and factor there are observable trends in permeability coefficients among the factors including the effects of astrocyte and pericyte cell density. With extended culturing, higher seeding densities of astrocytes and pericytes result in higher permeability of the dextran (Fig. 3). HBEC-5i seeding

density also shows trends towards lower permeability at higher seeding densities; however, this trend is not as strong at day 9 when the cells have had sufficient time to reach confluence and have a longer time to differentiate.

Using JMP 13.2 software, a prediction profiler was generated based on the obtained P_{eff} values for the given conditions. By maximizing Desirability to achieve the lowest possible permeability, the optimal conditions were determined to be 20,000 cells/cm^2 for both astrocytes and pericytes, 80,000 cells/cm^2 HBEC-5i cells, Matrigel® as the ECM protein, and culturing for 9 days post endothelial cell plating (Fig. 4). These conditions would optimally generate a predicted P_{eff} value of 2.4 x 10^{-6} cm/sec for 4 kD dextran. Upon repeating the analysis at selected optimal conditions, the P_{eff} of a 4 kD dextran showed to be reproducible resulting in a similar permeability value (P_{eff}; 3.7 x 10^{-6} cm/sec ± 0.04, n = 3).

Medium Optimization ($DOE_{M1/2}$)

Selection of medium additives was based on literature and previous studies in our laboratory for HBEC-5i medium based on their reported influences on barrier tightness both *in vitro* and *in vivo*.(51–58) The first DOE analysis of medium variables aimed towards optimization (DOE_{M1}) was performed with the DOE_P optimized plating conditions of 20,000 cells/cm^2 for astrocytes and pericytes, 80,000 cells/cm^2 HBEC-5i, Matrigel, after 9 days of endothelial growth. HEPES, hydrocortisone, dexamethasone, lithium chloride, calcium, and retinoic acid were used as medium additives due their reported influence on tight junction expression and induction of barrier properties in *in vitro* BBB models. The lowest achieved 4 kD dextran P_{eff} of DOE_{M1} was 6.3 x 10^{-6} cm/sec, suggesting that, under these conditions, the additives did not provide further tightening of the model. Significant trends are not apparent for any of the additives with the exception of higher levels of HEPES resulting in higher

342 permeability values. Given that many of these additives increased expression and differentiation
343 of the endothelial cells, their effects on barrier properties were assessed at earlier days of culture.
344 The optimal medium condition was determined to be 15 mM HEPES, 1 mM calcium, and 10 μM
345 retinoic acid, but the influence of these factors on barrier tightness was not significant (Fig. 5).
346 The full data set of DOE_{M1}, including medium conditions and P_{eff}, is tabled in Additional File 2.

347 Based on these results a second analysis (DOE_{M2}) was performed to assess the influence
348 of the additives in earlier days of culture. These studies were conducted in the presence or
349 absence of hydrocortisone, dexamethasone, lithium chloride, and retinoic acid at 5 and 7 days
350 post endothelial cell culture, HEPES was held constant at 15 mM and calcium was removed from
351 DOE_{M2}. The lowest 4 kD dextran P_{eff} of DOE_{M2} was 8.3 x 10^{-6} cm/sec, suggesting that the
352 additives do not provide increased barrier tightness based on the optimized plating conditions of
353 DOE_P. Optimal conditions for medium was determined to be 10 μM dexamethasone, 10 μM
354 retinoic acid, 10 mM LiCl, through 7 days of endothelial cell culture; however, these conditions
355 were not used for continued assessment of the optimized model due to the lack of improvement
356 over unmodified medium (Fig. 6). The complete data set of DOE_{M2}, including individual run and
357 P_{eff} results, can be found in Additional File 3.

358 **Permeation Comparisons to Mono- and Cocultures**

359 The optimized direct contact triculture was compared to a monoculture of HBEC-5i cells
360 alone and direct contact cocultures of HEBC-5i cells seeded atop a lawn of astrocytes or
361 pericytes (Fig. 7A). Effective permeability of the 4 kD FITC-dextran was used for comparison
362 between the different models. In comparison to the optimized direct contact triculture (3.7 x 10^{-6}
363 ± 0.0 cm/sec) the HBEC-5i monoculture had the highest observed permeability (19.7 x 10^{-6} ± 3.0
364 cm/sec; $p < 0.01$), followed by the perictye-HBEC-5i coculture (15.1 x 10^{-6} ± 3.7 cm/sec; $p <$

365 0.05), and the astrocyte-HBEC-5i coculture (12.8 x 10^{-6} ± 2.1 cm/sec; $p < 0.05$). Given the
366 significant differences observed between the direct contact triculture and the monoculture and
367 coculture models, the inclusion of all three cell types offers increased barrier tightness for the *in*
368 *vitro* model.

369 **Direct Contact Triculture BBB Marker Compounds**

370 Paracellular markers possessing a broad range of hydrodynamic radii were used to
371 evaluate the functional tightness of the optimized model (Fig. 7B).(59–61) The lowest apparent
372 paracellular permeability observed was that of PEG-4000 (7.85 x 10^{-6} ± 0.03 cm/sec, 15.9 Å)
373 followed by inulin (P_{app} = 15.53 x 10^{-6} ± 0.15 cm/sec, 10 Å), mannitol (P_{app} = 19.88 x 10^{-6} ± 0.07
374 cm/sec, 4.3 Å), and sucrose (P_{app} = 21.76 x 10^{-6} ± 0.17 cm/sec, 5.2 Å). The apparent paracellular
375 permeability of the hydrophilic markers shows the model is able to distinguish between markers
376 of varying sizes. However, based on the hydrodynamic radius, sucrose should have a lower
377 permeability as the larger compound in comparison to mannitol.

378 P-gp function in the direct contact triculture was assessed using P-gp substrate R123
379 alone and in the presence of P-gp inhibitor elacridar (Fig. 7C). In the absence of inhibitor, the
380 P_{app} of R123 was 18.52 x 10^{-6} ± 0.58 cm/sec. The presence of elacridar significantly increased
381 the P_{app} of R123 (P_{app} = 21.14 x 10^{-6} ± 0.46 cm/sec; $p<0.01$) across the direct contact triculture.
382 Additional P-gp substrates were utilized as marker compounds such as digoxin (P_{app} = 9.21 x 10^{-6}
383 ± 0.31 cm/sec) and colchicine (P_{app} = 18.67 x 10^{-6} ± 2.75 cm/sec). Prazosin, a BCRP substrate,
384 was used to assess the function of other efflux transporters in the direct contact model (P_{app} =
385 6.16 x 10^{-6} ± 0.11 cm/sec) (Fig. 8).

386 The antipsychotic drug clozapine showed an apparent permeability value of 8.15 x 10^{-6} ±
387 0.58 cm/sec. The amino acid L-histidine was used to assess facilitative transport across the *in*

388 *vitro* model with an observed apparent permeability of 52.61 x 10^{-6} ± 0.70 cm/sec, as reported
389 previously.(60) Carbamazepine is an antiepileptic drug and a BBB positive permeant with an
390 observed apparent permeability of 27.71 x 10^{-6} ± 1.13 cm/sec in the optimized model. Caffeine, a
391 small hydrophilic molecule, also had BBB positive permeation with an obtained apparent
392 permeability of 28.93 x 10^{-6} ± 1.15 cm/sec (Fig. 8).

393 ## Discussion

394 *In vitro* screening models have traditionally been used to evaluate the potential of new
395 chemical entities to cross the BBB, with much of the emphasis of these models being placed on
396 the endothelial cell type. The BMEC used is often primary or immortalized and of animal or
397 human origin, each presenting its own advantages for use in *in vitro* models.(30,62) Although
398 animal sources are typically lower cost, have significantly higher access, and can be easier to
399 isolate, physiological and phenotypic differences between the human and animal NVU make
400 human cell sources preferred for drug permeability screening due to the presumed physiological
401 relevance to the patient. Primary cells, directly isolated from patients, often present a phenotype
402 most similar to *in vivo*, but are often difficult to acquire due to ethical reasons, require intricate
403 isolation protocols, and present concerns with patient specific differences.(63,64) Therefore,
404 much of the emphasis has been placed on establishing and characterizing human immortalized
405 cell lines for robust screening methods.

406 The HBEC-5i cell line has not been as extensively used for *in vitro* BBB permeability
407 modeling comparative to other BMEC cell sources (e.g., hCMEC/D3).(60) However, it has been
408 shown to have good expression levels of brain endothelial markers such as vascular cell adhesion
409 molecule (VCAM-1) and intercellular adhesion molecule (ICAM-1) essential for immune cell
410 trafficking, CD51 (α_V-integrin) involved in extracellular matrix adhesion, as well as tight

411 junction proteins zonula occluden 1 (ZO-1) and claudin-5.(35,39) Transporter expression and
412 function of BCRP, P-gp, MRP-1, and MRP-2 has also been demonstrated recently to be
413 comparable to other immortalized brain endothelium.(39) Conversely, this cell line has also been
414 indicated to be lacking in expression of platelet endothelial cell adhesion molecules (PECAM-1
415 and CD31) and the macrophage scavenger receptor CD36.(35,65) Given the expression of
416 endothelial markers and transporters that have been investigated by others, we selected the
417 HBEC-5i cell line as the BMEC for the direct contact triculture rather than the hCMEC/D3 cell
418 line we utilized in development of the direct contact coculture.(51)

419 *In vitro* models of the BBB are increasingly being developed to provide physiological
420 relevance through co- and triculture indirect contact methods with astrocytes and pericytes that
421 comprise the NVU to further enhance barrier properties. Seeding supporting NVU cells on the
422 reverse side of the filter support displays improved barrier properties in the cultured BMECs by
423 reducing the distance between the cell types and improving the BBB phenotype in the cultured
424 endothelium.(50,66) However, the direct cell-cell contact is limited due to the thickness of the
425 filter support and opposable culturing surfaces, where growth through the filter pores provides
426 limited interaction. The direct cell-cell contacts of astrocytes and pericytes with the endothelium
427 *in vivo* are often overlooked in these multi-cellular models that are currently utilized.(30,41–45)
428 We have previously shown that direct contact between astrocytes and the endothelium in a
429 coculture model increases the barrier properties compared to endothelial monocultures and
430 indirect plating methods.(51) Although astrocytes are often used as a supporting cell in *in vitro*
431 models, pericytes also play an important role in influencing and regulating the BBB phenotype
432 through a number of signaling cascades.(24,67,68) Since each supporting cell acts in a
433 functionally different manner on the BMECs, incorporating both astrocytes and pericytes in

direct contact cell based models should better enable synergistic effects of the NVU to be represented *in vitro*.

A design of experiments approach was taken to develop and optimize the direct contact triculture in order to adequately understand the interactions each variable would have on the performance of the model. As opposed to an OFAT approach, DOE takes into account the implications of changing multiple variables to come to optimal conditions in a significantly more efficient manner in terms of time invested and resources required. In optimizing the triculture, we arrived at optimal conditions with reproducible results in a time frame of two months as opposed to our previous OFAT optimization efforts that spanned the course of multiple years. The results of DOE_P revealed optimal plating conditions of 20,000 cells/cm^2 for both astrocytes and pericytes, 80,000 cells/cm^2 for HBEC-5i, Matrigel® as the ECM to promote endothelial adhesion, and culturing the endothelium for 9 days after seeding. The comparison of 4 kD dextran permeability to other reported data revealed that our optimized model infers that the model is among the tightest we found reported, suggesting that culturing multiple NVU cell types in direct contact synergistically increases barrier tightness (Table 5).

Table 5. Peff Values of 4 kD Dextran (14 Å) for different BBB models.

Model/Endothelial Cell Line	**Peff (10^{-6} cm/sec)**
DOE Direct Contact Triculture, HBEC-5i	3.7
Monoculture (HA conditioned medium), HBEC-5i	3.6[a]
Monoculture, hCMEC/D3	8.8[b], 5.4[c]
Isolated endothelial cells, rat	1.0[d]
In vivo microvessels, rat	0.92[e]

[a]Puech, C., *et al.*, Int J Pharm (2018) 551(1) 281-289, [b]Förster, C., *et al.*, J Physiol (2008) 589(7) 1937-1949, [c]Weksler, B., *et al.*, FASEB J. (2005) 19(13) 1872-1874, [d]Watson, P.M.D., *et al.*, BMC Neuroscience (2013) 14:59, [e]Yuan, W.. *et al.*, Microvasc Res (2009) 77(2) 166-173

In addition to selecting an optimized set of plating conditions, the DOE approach facilitated an understanding of how changing factor levels may impact model performance. At higher densities of astrocytes and pericytes, a decrease in paracellular tightness was observed with extended culture time. Length of culturing time will vary with each individual endothelial cell line seeded in combination with the astrocytes and pericytes in culture and should be optimized based on the increase in tightness as an indicator of differentiation. However, the endothelial culture times do need to take into account whether or not the co-cultured astrocytes and pericytes maintain viability or run the risk of becoming senescent at the latter stages of the study. Additionally, higher seeding densities of endothelial cells resulted in lower paracellular permeation rates at days 5 and 7, which may be expected by the increased ability of the cells to form a confluent layer at fewer days of culture. However, that trend is less drastic after 9 days of culture suggesting that seeding density does not play as significant of a role at confluency, but rather time in culture is necessary to allow for differentiation and adequate tight junction formation.

An effort to optimize culture medium (DOE_{M1} and DOE_{M2}) was made to further increase barrier properties of the model through the inclusion of additives that have been shown to enhance the BBB phenotype in *in vitro* and *in vivo* studies. Unmodified HBEC-5i medium contains 15 mM HEPES; therefore, higher levels of HEPES were included to assess the impact of a higher buffering capacity on barrier tightness. Hydrocortisone was selected for its influence on inflammatory responses as a glucocorticoid and potential to prevent tight junction break down.(52) Lithium chloride has been shown to influence claudin expression through stimulation of the Wnt/β-catenin pathway.(53) Calcium was studied as a medium additive due to its influence on adherens and tight junction protein expression to increase barrier tightness, where

studies have shown that low extracellular calcium levels can lead to an increase in paracellular permeability.(54,55) Like hydrocortisone, dexamethasone acts to inhibit inflammatory responses and upregulate tight junctions; however, it is a synthetic alternative to the naturally occurring hydrocortisone.(56) Lastly, retinoic acid is naturally secreted by glial cells and has revealed significant increases in paracellular tightness in *in vitro* BBB models.(57,58)

Between both assessments it was revealed that the length of culture time for the endothelium still had the largest impact on model performance regardless of additives (Fig. 6). Based on this finding it is possible that due to the influence the additives have on the endothelium the HBEC-5i cells are differentiating before reaching confluency which is not sustainable through the length of culture. This phenomenon could also explain why the effects of additives appear to be more effective in DOE_{M2}, culturing for 5 or 7 days post endothelial plating, as the differentiation effects may be occurring earlier and not maintained through culture times for DOE_{M1}. A way to improve on this would be to include HBEC-5i seeding density as a factor in further assessments of medium additives. With the trends of DOE_P establishing the positive impacts higher seeding densities have on model tightness, seeding at a higher density (greater than the optimized 80,000 cells/cm^2) with differentiation inducing medium supplements may result in the tightest barrier formed and additionally reduce culturing time. An alternative would be to continue with optimized conditions of DOE_P and include time of addition as a factor in further studies by introducing additives after the HBEC-5i have been in culture for more than 24 hours.

The influence of the medium additives may also extend beyond paracellular tightness. Hydrocortisone has been shown to increase barrier tightness through the upregulation of tight junction proteins, but has also been demonstrated to induce efflux transporter

expression.(39,69,70) Expression and function of ABC efflux transporters, specifically BCRP and P-gp, was also demonstrated to be influenced by the release of tumor necrosis factor-α (TNF-α) and subsequent inflammatory responses.(39,70,71) However, hydrocortisone is a glucocorticoid that has been demonstrated to impact P-gp and BCRP expression by inducing anti-inflammatory responses. Therefore, in addition to the impact on paracellular tightness, the induction of efflux transporter expression should also be assessed by evaluating the time of addition of hydrocortisone to the culture medium.

The increase in physiological relevance of adding additional cell types of the NVU in direct contact with BBB endothelium provides increased barrier restrictive properties in comparison to the endothelium alone. Additionally, including both supporting cell types (astrocytes and pericytes) in direct contact with HBEC-5i cells results in increased barrier tightness compared to direct contact cocultures (astrocyte- or pericyte-HBEC 5i combinations alone). This finding suggests that including both the astrocytes and pericytes in *in vitro* models further synergistically enhances the properties of the BBB in addition to better representing the *in vivo* NVU. The inductive effects of astrocytes and pericytes and their roles in BBB maintenance have been well established; however, many of the models used for *in vitro* BBB permeability screening do not consider the direct contact the different cell types have with one another *in vivo*. By seeding astrocytes, pericytes, and the endothelium directly atop one another this model better mimics the 20 nm distance between the cell types due to the presence of the basal lamina that is seen *in vivo*.(22) Although indirect plating methods with cell types cultured on opposite sides of a 10 μm thick filter support also provide increased barrier properties over endothelial monocultures, the direct contact triculture is more physiologically relevant to the *in vivo* BBB that is observed in the NVU and does not require manipulation of the Transwell®

system and potentially is more amenable to automation for higher capacity throughput screening assays.

Paracellular permeants of increasing hydrodynamic radius were selected to evaluate the tight junction formation in the direct contact model. With increasing marker size, there is a related decrease in paracellular permeability due to the size of the molecule in relation to the pore size of the tight junctions formed between adjacent endothelial cells. Permeability of [^{14}C]-PEG-4000 (15.9 Å) is the lowest of all markers used as expected followed by [^{14}C]-inulin (10 Å). In studies with the optimized direct contact triculture model, the permeability of [^{14}C]-sucrose (5.2 Å) is faster than that of the smaller [^{14}C]-mannitol (4.3 Å), which is opposite of what would be expected based on molecule size alone.(59–61) One possible explanation is that the relative size of the two markers is small in comparison to the paracellular pore radius in the triculture model, which would lead to issues in elucidating the differences in their respective permeation rates as they both traverse relatively fast. Alternatively, sucrose, a disaccharide of a fructose and glucose molecule linked via glycosidic bond, may serve as a substrate for active or facilitative nutrient transporters. For example, glucose permeation across the BBB has been reported to be modulated by several nutrient transporters, in particular the facilitative Glucose Transporter 1 (GLUT1) that is highly expressed in both BMECs and astrocytes.(72,73) Several neurotherapeutics utilize a pro-drug approach where the agent is conjugated to glucose in an effort to enhance brain parenchymal exposure via GLUT1.(72,74) Based on the structure of sucrose, the idea that there is some degree of nutrient transporter activity of the purported paracellular marker via the GLUT1 transporter is feasible. Therefore, we posit that the observed permeation rate for sucrose could be higher due to a potential transporter contribution that is not available for [^{14}C]-mannitol in the optimized direct contact triculture. This theory is further

548 exacerbated by the presence of astrocytes and pericytes on the apical side of the Transwell® in
549 the direct contact triculture since both of these cell types have reported expression of GLUT1.
550 The potential for GLUT1 mediated transport and a potential increase the permeation of [^{14}C]-
551 sucrose in the apical to basolateral direction in comparison to indirect *in vitro* models requires
552 further investigation. Future studies might focus on delineating the effects GLUT1, a related
553 transporter, with co-administration of transporter inhibitors, or with GLUT isoform transfected
554 HBEC-5i cells.

555 The functional activity of ATP-Binding Cassette efflux transporters, with the most
556 prevalent isoform being P-gp, in BMECs is a key characteristic of the *in vivo* BBB. P-gp, BCRP,
557 and related multidrug resistance conferring efflux transporters function to prevent xenobiotics
558 from permeating into the brain parenchyma with a broad substrate affinity and capacity.
559 Rhodamine-123 (R123) is a commonly used P-gp substrate to assess functional activity in the
560 presence or absence of an inhibitor. Elacridar is a third generation P-gp inhibitor and has been
561 reported to have among the highest specificity and potency for P-gp inhibition within the class of
562 agents.(75) We observed that the presence of elacridar resulted in an increase in R123
563 permeability across the direct contact triculture, suggesting that P-gp is functionally present in
564 the optimized model. In these studies, R123 permeation was only assessed in the apical to
565 basolateral direction. Additional studies to elucidate P-gp function can include bi-directional
566 permeability assessment as well as cellular accumulation. However, given that P-gp is expressed
567 in both the HBEC-5i and astrocyte cell types in direct contact, the assessment of P-gp function
568 and expression would require more in depth studies focused on delineating the impact of P-gp in
569 each cell and in combination. This is particularly true given the fact that astrocytes have also

been reported to express P-gp, which may further obfuscate P-gp assessment of the endothelium alone.(76)

In addition to limiting paracellular permeation of hydrophilic solutes and potentially P-gp substrates, we theorized that a well-established *in vitro* model of the BBB found in the NVU should have an enhanced ability to differentiate between *in vivo* demonstrated high and low brain permeating compounds. *In vitro* permeability screening models capable of predicting *in vivo* permeation rates in order to rank new chemical entities is essential to facilitate compound advancement with translation as the aim.(77,78) A number of positive and negative permeants were selected to assess the utility of the direct contact triculture. Amino acids and related analogues (e.g. γ-aminobutyric acid or GABA) play a critical role in maintaining brain homeostasis and modulating function. Here we selected L-histidine as an amino acid that is actively transported in a stereospecific manner across the BBB by amino acid transporters and potentially Peptide Histidine Transporter 1.(60,79) However, L-histidine is a small water soluble molecule that can potentially permeate *in vitro* models to an extent via the paracellular pathway. Hence, the paracellular route cannot be ignored as it may contribute to a higher permeation rate of L-histidine in comparison to other transporter specific markers. Caffeine was also selected as a small hydrophilic psychostimulant that has been demonstrated to permeate the *in vivo* BBB, and we demonstrated its permeation across the direct contact triculture model.(80) Carbamazepine was selected as it is an anticonvulsant commonly used as a BBB positive marker and to our knowledge has not been shown to possess significant P-gp affinity.(81,82) In addition to R123, permeability of P-gp substrates colchicine and digoxin were assessed in the optimized model. The differences in permeation rates for separate P-gp substrates can be attributed to the broad substrate affinities and capacities of the efflux transporters and their relative expression

levels. Further studies can be performed to assess the effect of P-gp inhibition on the permeation of these substrates as well as inhibition of other efflux transporters such as BCRP as there is also fairly significant substrate overlap across several efflux transporter isoforms. Clozapine is an antipsychotic that has been shown to be highly metabolized and may potentially inhibit P-gp.(69,83) Clozapine metabolites have also been demonstrated to have high BBB permeation, where additional studies using LC-mass spectrometry analysis and longer incubation time could be performed to elucidate the metabolic fate in the optimized triculture model.(83) Although, it is important to note that there were no metabolite peaks observed in the chromatograms during the time course of this study. Lastly, prazosin is a BCRP substrate that proved to have the lowest permeability of the selected markers. The low permeation of prazosin across the *in vitro* triculture model potentially suggests that functional BCRP activity is greater than that of P-gp or other efflux transporters, however further studies need to be performed to delineate the effects. The observed ranking of high and low BBB permeating compounds is ordered in a similar fashion to what has been seen by others both *in vitro* and *in vivo*.(84,85) The observed permeability of a small library of compounds across the optimized direct contact triculture model suggests that it is a useful tool for further assessment of BBB permeation of new chemical entities as well understanding of the synergistic effects of direct cell-cell contacts.

Conclusion

Herein, we have established an enhanced physiologically relevant *in vitro* model of the BBB by culturing the astrocytes, pericytes, and HBEC-5i cells in a layered, direct contact manner similar to the *in vivo* BBB that is comprised as part of the NVU. We provide supporting evidence that apical cell layering removes the physical filter barrier observed in conventional triculture models and supports the potential of synergistic interactions occurring to provide a phenotype closer to the NVU. In addition, to our knowledge we are one of the first laboratories

to utilize a three-stage multifactorial DOE based approach to expedite optimization of a BBB *in vitro* model. It is recommended that additional DOE based studies be performed to develop analogous models to mimic different pathologies of the brain, for example neurodevelopmental changes or neurodegenerative effects on the BBB with primary or proliferative cell lines.

The Blood Brain Barrier *in vitro* screening approaches have traditionally focused on tightening the brain microvessel endothelium that lines the capillaries, separates the blood from the neuronal environment, and maintains homeostasis. While screening models in the presence of astrocytes and pericytes in indirect contact to the BMECs have been developed, we postulated that direct contact of these cells, as found *in vivo*, would more adequately enhance *in vitro-in vivo* comparative studies. The direct layered culturing approach should enhance the synergistic effects by removing physical barriers and providing proximity so that secreted soluble factors and their effects on the regulation of the BMEC phenotype should be enhanced without added dilution and diffusion. Additionally, the ability for the model to rank established high and low brain permeating compounds alludes to its potential for BBB permeability screening of new chemical entities. This study also demonstrates the feasibility of using an informed DOE based approach to expedite culture development and can be further expanded for additional applications. Taken together, the direct contact triculture developed within appears to provide increased barrier properties that we theorize is attributable through facilitating adequate crosstalk between the three major cell types of the BBB that aids in the formation of the *in vivo* NVU. The findings of this work open the door for continued investigation of the roles of each BBB and potentially NVU cell type and its influence on barrier properties, as well as the establishment of a fully human, physiologically relevant *in vitro* model that can be used for moderate throughput screening to rank order potential neurotherapeutic compounds.

Abbreviations

ABC – ATP binding cassette

BBB – blood brain barrier

BCRP – breast cancer resistant protein

BMEC – brain microvessel endothelial cell

DMEM/F-12 – Dulbecco's Modified Eagle Medium/Nutrient Mixture F-12

DMSO – dimethylsulfoxide

DOE – design of experiments

ECGS – endothelial cell growth supplement

ECM – extracellular matrix

FBS – fetal bovine serum

FITC – Fluorescein isothiocyanate

GLUT-1 – glucose transporter 1

HBSS – Hank's balanced salt solution

HBEC-5i – human brain endothelial cell

hCMEC/D3 – human cerebral microvessel endothelial cell

HEPES – 2-[4-(2-hydroxyethyl)piperazin-1-yl]ethanesulfonic acid

ICAM-1 – intercellular adhesion molecule 1

NVU – neurovascular unit

OFAT – one factor at a time

Papp – apparent permeability

PBS – phosphate buffered saline

PDGF-B – platelet-derived growth factor B

Peff – effective permeability

PECAM-1 – platelet endothelial cell adhesion molecule 1

P-gp – p-glycoprotein

PLL – poly-L-lysine

R123 – rhodamine 123

TEER – transendothelial electrical resistance

TGF-β – transforming growth factor-β

TNF-α – tumor necrosis factor- α

VCAM-1 – vascular adhesion molecule 1

ZO-1 – zonula occluden 1

Declarations

Ethics approval and consent to participate

'Not applicable'

Consent for publication

'Not applicable'

Availability of data and materials

All data generated or analyzed during this study are included in this published article and its Additional Files.

Competing interest

Authors KL and GK are inventors under US Patent No. 10877026 which covers the work presented in this publication.

Funding

685 This work was supported in part by Environmental Protection Agency OSAPE Star Grant #RD-
686 84002701-0.

687 **Authors' contributions**

688 KL designed and performed the experiments. KL and GK analyzed the data and drafted,
689 reviewed, and approved the manuscript.

690 **Acknowledgements**

691 The authors would like to acknowledge their co-inventors of US Patent No. 10877026 Dr.
692 Christopher D. Kulczar, Dr. Monika Lavan, and Dr. Aimable Ngendahimana for their
693 contributions to the establishment of this model.

694 ## Figure Captions

695 **Figure 1.** Cross sectional depiction of the Blood-Brain Barrier within the neurovascular unit
696 (NVU) with the endothelium (BMECs) lining the capillary, pericytes embedded within the basal
697 lamina, astrocytes having nearly full coverage of the BMECs and surrounding pericytes, and
698 neurons in close contact with the astrocytes (left). The direct contact triculture model on the
699 apical surface of a Transwell® filter support mimicking the *in vivo* NVU. Astrocytes are seeded
700 first on the filter, followed by pericytes, then BMECs to generate a fully apical, direct contact
701 triculture model (right).

702 **Figure 2.** P_{app} and P_{eff} of 4 kD FITC-Dextran across different direct contact triculture conditions
703 of DOE_P. All DOE_P selected conditions were performed as n=1 for a rapid evaluation of the
704 different parameter combinations. Condition 13 was compromised and permeability was not
705 performed, data point was excluded from statistical analysis.

706 **Figure 3.** P_{eff} of 4 kD FITC-Dextran for DOE_P separated by factor and further by day of study
707 showing relative trends of factor levels at increasing length of culture. All conditions are
708 represented by single data points across the graph, n=1.
709 **Figure 4.** JMP 13.2 Prediction Profiler generated based on maximizing desirability for P_{eff} based
710 on DOE_P. Optimal plating conditions 20,000 cells/cm^2 astrocytes and pericytes, 80,000 cells/cm^2
711 HBEC-5i, Matrigel, and 9 days of endothelial growth. Predicted P_{eff} of 2.4 x 10^{-6} cm/sec for
712 optimal conditions.
713 **Figure 5.** JMP 13.2 Prediction Profiler generated based on maximizing desirability for P_{eff} of
714 DOE_{M1}. Optimal medium conditions 15 mM HEPES, 1 mM Ca^{2+}, and 10 µM retinoic acid at 9
715 days of endothelial growth. Predicted P_{eff} of 7.0 x 10^{-6} cm/sec for optimal conditions.
716 **Figure 6.** JMP 13.2 Prediction Profiler generated based on maximizing desirability for P_{eff} of
717 DOE_{M2}. Optimal medium conditions 10 µM dexamethasone, 10 µM retinoic acid, 10 mM LiCl,
718 through 7 days of endothelial culture. Predicted P_{eff} of 8.8 x 10^{-6} cm/sec for optimal conditions.
719 **Figure 7. Optimized Triculture Permeability. (A)** Effective permeability (P_{eff}) of 4 kD FITC-
720 dextran across an HBEC-5i monoculture, pericyte-HBEC-5i direct contact coculture, astrocyte-
721 HBEC-5i direct contact coculture, and optimized direct contact triculture. Statistical analysis was
722 performed with one-way ANOVA and Tukey-Kramer post-hoc test. Error bars represent one
723 standard deviation (n=3). *, $p < 0.05$ and **, $p < 0.01$. **(B)** Apparent permeability of radiolabeled
724 paracellular markers [^{14}C]-sucrose. [^{14}C]-mannitol, [^{14}C]-inulin, and [^{14}C]-PEG-4000 across the
725 optimized direct contact triculture. Error bars represent one standard deviation (n=3). (C)
726 Apparent permeability of P-gp substrate rhodamine 123 (R123) in the presence and absence of P-gp
727 inhibitor elacridar across the optimized direct contact triculture. Assays were run in triplicate and
728 subjected to Student's *t*-test. Significant difference is indicated by *, $p < 0.05$ and **, $p < 0.01$. Error bars
729 represent one standard deviation (n=3).

Figure 8. Apparent permeability of BBB positive (L-histidine, carbamazepine, and rhodamine 123 in the presence of P-gp inhibitor elacridar) and negative (colchicine, rhodamine 123, digoxin, clozapine, and prazosin) permeants across the optimized direct contact triculture. Assays were performed in triplicate. Error bars represent one standard deviation (n=3).

References

1. Pardridge WM. Why is the global CNS pharmaceutical market so under-penetrated? Drug Discov Today. 2002 Jan 1;7(1):5–7.
2. Gribkoff VK, Kaczmarek LK. The Need for New Approaches in CNS Drug Discovery: Why Drugs Have Failed, and What Can Be Done to Improve Outcomes. Neuropharmacology. 2017 Jul 1;120:11–9.
3. Kesselheim AS, Hwang TJ, Franklin JM. Two decades of new drug development for central nervous system disorders. Nat Rev Drug Discov. 2015 Dec;14(12):815–6.
4. Abbott NJ, Patabendige AAK, Dolman DEM, Yusof SR, Begley DJ. Structure and function of the blood-brain barrier. Neurobiol Dis. 2010 Jan;37(1):13–25.
5. Abbott NJ. Blood-brain barrier structure and function and the challenges for CNS drug delivery. J Inherit Metab Dis. 2013 May;36(3):437–49.
6. Serlin Y, Shelef I, Knyazer B, Friedman A. Anatomy and Physiology of the Blood-Brain Barrier. Semin Cell Dev Biol. 2015 Feb;38:2–6.
7. Weiss N, Miller F, Cazaubon S, Couraud P-O. The blood-brain barrier in brain homeostasis and neurological diseases. Biochim Biophys Acta BBA - Biomembr. 2009 Apr;1788(4):842–57.
8. Bauer H-C, Krizbai IA, Bauer H, Traweger A. "You Shall Not Pass"-tight junctions of the blood brain barrier. Front Neurosci. 2014;8:392.
9. Haseloff RF, Dithmer S, Winkler L, Wolburg H, Blasig IE. Transmembrane proteins of the tight junctions at the blood-brain barrier: structural and functional aspects. Semin Cell Dev Biol. 2015 Feb;38:16–25.
10. Wolburg H, Lippoldt A. Tight junctions of the blood-brain barrier: development, composition and regulation. Vascul Pharmacol. 2002 Jun;38(6):323–37.
11. Löscher W, Potschka H. Blood-brain barrier active efflux transporters: ATP-binding cassette gene family. NeuroRx J Am Soc Exp Neurother. 2005 Jan;2(1):86–98.
12. Polli JW, Olson KL, Chism JP, John-Williams LS, Yeager RL, Woodard SM, et al. An Unexpected Synergist Role of P-Glycoprotein and Breast Cancer Resistance Protein on the

Central Nervous System Penetration of the Tyrosine Kinase Inhibitor Lapatinib (N-{3-Chloro-4-[(3-fluorobenzyl)oxy]phenyl}-6-[5-({[2-(methylsulfonyl)ethyl]amino}methyl)-2-furyl]-4-quinazolinamine; GW572016). Drug Metab Dispos. 2009 Feb 1;37(2):439–42.

13. Abbott NJ, Rönnbäck L, Hansson E. Astrocyte-endothelial interactions at the blood-brain barrier. Nat Rev Neurosci. 2006 Jan;7(1):41–53.

14. Bouchaud C, Le Bert M, Dupouey P. Are close contacts between astrocytes and endothelial cells a prerequisite condition of a blood-brain barrier? The rat subfornical organ as an example. Biol Cell. 1989;67(2):159–65.

15. Bushong EA, Martone ME, Jones YZ, Ellisman MH. Protoplasmic astrocytes in CA1 stratum radiatum occupy separate anatomical domains. J Neurosci Off J Soc Neurosci. 2002 Jan 1;22(1):183–92.

16. Halassa MM, Fellin T, Takano H, Dong J-H, Haydon PG. Synaptic islands defined by the territory of a single astrocyte. J Neurosci Off J Soc Neurosci. 2007 Jun 13;27(24):6473–7.

17. Wolburg H, Wolburg-Buchholz K, Fallier-Becker P, Noell S, Mack AF. Chapter one - Structure and Functions of Aquaporin-4-Based Orthogonal Arrays of Particles. In: Jeon KW, editor. International Review of Cell and Molecular Biology [Internet]. Academic Press; 2011 [cited 2018 Feb 12]. p. 1–41. Available from: http://www.sciencedirect.com/science/article/pii/B9780123860439000013

18. Haseloff RF, Blasig IE, Bauer HC, Bauer H. In search of the astrocytic factor(s) modulating blood-brain barrier functions in brain capillary endothelial cells in vitro. Cell Mol Neurobiol. 2005 Feb;25(1):25–39.

19. Lee S-W, Kim WJ, Choi YK, Song HS, Son MJ, Gelman IH, et al. SSeCKS regulates angiogenesis and tight junction formation in blood-brain barrier. Nat Med. 2003 Jul;9(7):900–6.

20. Argaw AT, Gurfein BT, Zhang Y, Zameer A, John GR. VEGF-mediated disruption of endothelial CLN-5 promotes blood-brain barrier breakdown. Proc Natl Acad Sci U S A. 2009 Feb 10;106(6):1977–82.

21. Alvarez JI, Katayama T, Prat A. Glial influence on the Blood Brain Barrier. Glia. 2013 Dec;61(12):1939–58.

22. Mathiisen TM, Lehre KP, Danbolt NC, Ottersen OP. The perivascular astroglial sheath provides a complete covering of the brain microvessels: An electron microscopic 3D reconstruction. Glia. 2010 Jul 1;58(9):1094–103.

23. Winkler EA, Bell RD, Zlokovic BV. Central nervous system pericytes in health and disease. Nat Neurosci. 2011 Oct 26;14(11):1398–405.

24. Daneman R, Zhou L, Kebede AA, Barres BA. Pericytes are required for blood-brain barrier integrity during embryogenesis. Nature. 2010 Nov 25;468(7323):562–6.

25. Gaengel K, Genové G, Armulik A, Betsholtz C. Endothelial-mural cell signaling in vascular development and angiogenesis. Arterioscler Thromb Vasc Biol. 2009 May;29(5):630–8.

26. Hawkins BT, Davis TP. The Blood-Brain Barrier/Neurovascular Unit in Health and Disease. Pharmacol Rev. 2005 Jun 1;57(2):173–85.

27. Baeten KM, Akassoglou K. Extracellular Matrix and Matrix Receptors in Blood-Brain Barrier Formation and Stroke. Dev Neurobiol. 2011 Nov;71(11):1018–39.

28. Weksler BB, Subileau EA, Perrière N, Charneau P, Holloway K, Leveque M, et al. Blood-brain barrier-specific properties of a human adult brain endothelial cell line. FASEB J Off Publ Fed Am Soc Exp Biol. 2005 Nov;19(13):1872–4.

29. Weksler B, Romero IA, Couraud P-O. The hCMEC/D3 cell line as a model of the human blood brain barrier. Fluids Barriers CNS. 2013 Mar 26;10(1):16.

30. Helms HC, Abbott NJ, Burek M, Cecchelli R, Couraud P-O, Deli MA, et al. In vitro models of the blood-brain barrier: An overview of commonly used brain endothelial cell culture models and guidelines for their use. J Cereb Blood Flow Metab Off J Int Soc Cereb Blood Flow Metab. 2016 May;36(5):862–90.

31. Tai LM, Reddy PS, Lopez-Ramirez MA, Davies HA, Male DK, Male ADK, et al. Polarized P-glycoprotein expression by the immortalised human brain endothelial cell line, hCMEC/D3, restricts apical-to-basolateral permeability to rhodamine 123. Brain Res. 2009 Oct 6;1292:14–24.

32. Biemans EALM, Jäkel L, de Waal RMW, Kuiperij HB, Verbeek MM. Limitations of the hCMEC/D3 cell line as a model for Aβ clearance by the human blood-brain barrier. J Neurosci Res. 2017 Jul;95(7):1513–22.

33. Urich E, Lazic SE, Molnos J, Wells I, Freskgård P-O. Transcriptional profiling of human brain endothelial cells reveals key properties crucial for predictive in vitro blood-brain barrier models. PloS One. 2012;7(5):e38149.

34. Dorovini-Zis K, Prameya R, Bowman PD. Culture and characterization of microvascular endothelial cells derived from human brain. Lab Investig J Tech Methods Pathol. 1991 Mar;64(3):425–36.

35. Wassmer SC, Combes V, Candal FJ, Juhan-Vague I, Grau GE. Platelets Potentiate Brain Endothelial Alterations Induced by Plasmodium falciparum. Infect Immun. 2006 Jan 1;74(1):645–53.

36. Wassmer SC, Cianciolo GJ, Combes V, Grau GE. Inhibition of Endothelial Activation: A New Way to Treat Cerebral Malaria? PLoS Med [Internet]. 2005 Sep [cited 2018 Apr 19];2(9). Available from: https://www.ncbi.nlm.nih.gov/pmc/articles/PMC1188254/

37. Jambou R, Combes V, Jambou M-J, Weksler BB, Couraud P-O, Grau GE. Plasmodium falciparum adhesion on human brain microvascular endothelial cells involves transmigration-like cup formation and induces opening of intercellular junctions. PLoS Pathog. 2010 Jul 29;6(7):e1001021.

38. Jiang W, Huang W, Chen Y, Zou M, Peng D, Chen D. HIV-1 Transactivator Protein Induces ZO-1 and Neprilysin Dysfunction in Brain Endothelial Cells via the Ras Signaling Pathway [Internet]. Oxidative Medicine and Cellular Longevity. 2017 [cited 2018 Nov 29]. Available from: https://www.hindawi.com/journals/omcl/2017/3160360/

39. Puech C, Hodin S, Forest V, He Z, Mismetti P, Delavenne X, et al. Assessment of HBEC-5i endothelial cell line cultivated in astrocyte conditioned medium as a human blood-brain barrier model for ABC drug transport studies. Int J Pharm. 2018 Nov 15;551(1):281–9.

40. Puech C, Delavenne X, He Z, Forest V, Mismetti P, Perek N. Direct oral anticoagulants are associated with limited damage of endothelial cells of the blood-brain barrier mediated by the thrombin/PAR-1 pathway. Brain Res. 2019 May 20;

41. Dohgu S, Takata F, Yamauchi A, Nakagawa S, Egawa T, Naito M, et al. Brain pericytes contribute to the induction and up-regulation of blood-brain barrier functions through transforming growth factor-beta production. Brain Res. 2005 Mar 21;1038(2):208–15.

42. Zozulya A, Weidenfeller C, Galla H-J. Pericyte-endothelial cell interaction increases MMP-9 secretion at the blood-brain barrier in vitro. Brain Res. 2008 Jan 16;1189:1–11.

43. Demeuse P, Kerkhofs A, Struys-Ponsar C, Knoops B, Remacle C, van den Bosch de Aguilar P. Compartmentalized coculture of rat brain endothelial cells and astrocytes: a syngenic model to study the blood–brain barrier. J Neurosci Methods. 2002 Nov 15;121(1):21–31.

44. Thanabalasundaram G, El-Gindi J, Lischper M, Galla H-J. Methods to assess pericyte-endothelial cell interactions in a coculture model. Methods Mol Biol Clifton NJ. 2011;686:379–99.

45. Li G, Simon MJ, Cancel LM, Shi Z-D, Ji X, Tarbell JM, et al. Permeability of endothelial and astrocyte cocultures: in vitro blood-brain barrier models for drug delivery studies. Ann Biomed Eng. 2010 Aug;38(8):2499–511.

46. Thomsen LB, Burkhart A, Moos T. A Triple Culture Model of the Blood-Brain Barrier Using Porcine Brain Endothelial cells, Astrocytes and Pericytes. PloS One. 2015;10(8):e0134765.

47. Wuest DM, Wing AM, Lee KH. Membrane configuration optimization for a murine in vitro blood–brain barrier model. J Neurosci Methods. 2013 Jan 30;212(2):211–21.

48. Hatherell K, Couraud P-O, Romero IA, Weksler B, Pilkington GJ. Development of a three-dimensional, all-human in vitro model of the blood–brain barrier using mono-, co-, and tri-cultivation Transwell models. J Neurosci Methods. 2011 Aug 15;199(2):223–9.

870 49. McConnell HL, Kersch CN, Woltjer RL, Neuwelt EA. The Translational Significance of
871 the Neurovascular Unit. J Biol Chem. 2017 Jan 20;292(3):762–70.

872 50. Malina KC-K, Cooper I, Teichberg VI. Closing the gap between the in-vivo and in-vitro
873 blood–brain barrier tightness. Brain Res. 2009 Aug 11;1284:12–21.

874 51. Kulczar C, Lubin KE, Lefebvre S, Miller DW, Knipp GT. Development of a direct contact
875 astrocyte-human cerebral microvessel endothelial cells blood-brain barrier coculture model.
876 J Pharm Pharmacol. 2017 Dec;69(12):1684–96.

877 52. Förster C, Burek M, Romero IA, Weksler B, Couraud P-O, Drenckhahn D. Differential
878 effects of hydrocortisone and TNFα on tight junction proteins in an in vitro model of the
879 human blood–brain barrier. J Physiol. 2008 Apr 1;586(Pt 7):1937–49.

880 53. Paolinelli R, Corada M, Ferrarini L, Devraj K, Artus C, Czupalla CJ, et al. Wnt Activation
881 of Immortalized Brain Endothelial Cells as a Tool for Generating a Standardized Model of
882 the Blood Brain Barrier In Vitro. PLOS ONE. 2013 Aug 5;8(8):e70233.

883 54. Brown RC, Davis TP. Calcium modulation of adherens and tight junction function: a
884 potential mechanism for blood-brain barrier disruption after stroke. Stroke. 2002
885 Jun;33(6):1706–11.

886 55. De Bock M, Culot M, Wang N, da Costa A, Decrock E, Bol M, et al. Low extracellular
887 Ca2+ conditions induce an increase in brain endothelial permeability that involves
888 intercellular Ca2+ waves. Brain Res. 2012 Dec 3;1487:78–87.

889 56. Hue CD, Cho FS, Cao S, "Dale" Bass CR, Meaney DF, Morrison III B. Dexamethasone
890 potentiates in vitro blood-brain barrier recovery after primary blast injury by glucocorticoid
891 receptor-mediated upregulation of ZO-1 tight junction protein. J Cereb Blood Flow Metab.
892 2015 Jul;35(7):1191–8.

893 57. Lippmann ES, Al-Ahmad A, Azarin SM, Palecek SP, Shusta EV. A retinoic acid-enhanced,
894 multicellular human blood-brain barrier model derived from stem cell sources. Sci Rep.
895 2014 Feb 24;4:4160.

896 58. Mizee MR, Wooldrik D, Lakeman KAM, Hof B van het, Drexhage JAR, Geerts D, et al.
897 Retinoic Acid Induces Blood–Brain Barrier Development. J Neurosci. 2013 Jan
898 23;33(4):1660–71.

899 59. Ghandehari H, Smith PL, Ellens H, Yeh PY, Kopecek J. Size-dependent permeability of
900 hydrophilic probes across rabbit colonic epithelium. J Pharmacol Exp Ther. 1997
901 Feb;280(2):747–53.

902 60. Carl SM, Lindley DJ, Das D, Couraud PO, Weksler BB, Romero I, et al. ABC and SLC
903 transporter expression and proton oligopeptide transporter (POT) mediated permeation
904 across the human blood--brain barrier cell line, hCMEC/D3 [corrected]. Mol Pharm. 2010
905 Aug 2;7(4):1057–68.

61. Sorensen M, Steenberg B, Knipp GT, Wang W, Steffansen B, Frokjaer S, et al. The effect of beta-turn structure on the permeation of peptides across monolayers of bovine brain microvessel endothelial cells. Pharm Res. 1997 Oct;14(10):1341–8.

62. NAIK P, CUCULLO L. In Vitro Blood–Brain Barrier Models: Current and Perspective Technologies. J Pharm Sci. 2012 Apr;101(4):1337–54.

63. Bernas MJ, Cardoso FL, Daley SK, Weinand ME, Campos AR, Ferreira AJG, et al. Establishment of primary cultures of human brain microvascular endothelial cells to provide an in vitro cellular model of the blood-brain barrier. Nat Protoc. 2010 Jul;5(7):1265–72.

64. Lacombe O, Videau O, Chevillon D, Guyot A-C, Contreras C, Blondel S, et al. In vitro primary human and animal cell-based blood-brain barrier models as a screening tool in drug discovery. Mol Pharm. 2011 Jun 6;8(3):651–63.

65. Knipp GT, Liu B, Audus KL, Fujii H, Ono T, Soares MJ. Fatty acid transport regulatory proteins in the developing rat placenta and in trophoblast cell culture models. Placenta. 2000 May;21(4):367–75.

66. Gaston JD, Bischel LL, Fitzgerald LA, Cusick KD, Ringeisen BR, Pirlo RK. Gene Expression Changes in Long-Term In Vitro Human Blood-Brain Barrier Models and Their Dependence on a Transwell Scaffold Material. J Healthc Eng [Internet]. 2017 [cited 2018 Apr 23];2017. Available from: https://www.ncbi.nlm.nih.gov/pmc/articles/PMC5727720/

67. Lai C-H, Kuo K-H. The critical component to establish in vitro BBB model: Pericyte. Brain Res Brain Res Rev. 2005 Dec 15;50(2):258–65.

68. Armulik A, Genové G, Mäe M, Nisancioglu MH, Wallgard E, Niaudet C, et al. Pericytes regulate the blood-brain barrier. Nature. 2010 Nov 25;468(7323):557–61.

69. Maines LW, Antonetti DA, Wolpert EB, Smith CD. Evaluation of the role of P-glycoprotein in the uptake of paroxetine, clozapine, phenytoin and carbamazapine by bovine retinal endothelial cells. Neuropharmacology. 2005 Oct 1;49(5):610–7.

70. Wedel-Parlow MV, Wölte P, Galla H-J. Regulation of major efflux transporters under inflammatory conditions at the blood-brain barrier in vitro. J Neurochem. 2009;111(1):111–8.

71. Eisenblätter T, Galla H-J. A new multidrug resistance protein at the blood-brain barrier. Biochem Biophys Res Commun. 2002 May 17;293(4):1273–8.

72. Patching SG. Glucose Transporters at the Blood-Brain Barrier: Function, Regulation and Gateways for Drug Delivery. Mol Neurobiol. 2017 Mar;54(2):1046–77.

73. Morgello S, Uson RR, Schwartz EJ, Haber RS. The human blood-brain barrier glucose transporter (GLUT1) is a glucose transporter of gray matter astrocytes. Glia. 1995 May;14(1):43–54.

74. Xiuli G, Meiyu G, Guanhua D. Glucose Transporter 1, Distribution in the Brain and in Neural Disorders: Its Relationship With Transport of Neuroactive Drugs Through the Blood-Brain Barrier. Biochem Genet. 2005 Apr 1;43(3):175–87.

75. Amin MdL. P-glycoprotein Inhibition for Optimal Drug Delivery. Drug Target Insights. 2013 Aug 19;7:27–34.

76. Zhang L, Ong WY, Lee T. Induction of P-glycoprotein expression in astrocytes following intracerebroventricular kainate injections. Exp Brain Res. 1999 Jun;126(4):509–16.

77. Wang Q, Rager JD, Weinstein K, Kardos PS, Dobson GL, Li J, et al. Evaluation of the MDR-MDCK cell line as a permeability screen for the blood-brain barrier. Int J Pharm. 2005 Jan 20;288(2):349–59.

78. Hidalgo IJ. Assessing the absorption of new pharmaceuticals. Curr Top Med Chem. 2001 Nov;1(5):385–401.

79. Yamakami J, Sakurai E, Sakurada T, Maeda K, Hikichi N. Stereoselective blood-brain barrier transport of histidine in rats. Brain Res. 1998 Nov 23;812(1–2):105–12.

80. Chen X, Ghribi O, Geiger JD. Caffeine protects against disruptions of the blood-brain barrier in animal models of Alzheimer's and Parkinson's disease. J Alzheimers Dis JAD. 2010;20(Suppl 1):S127–41.

81. Grewal GK, Kukal S, Kanojia N, Madan K, Saso L, Kukreti R. In Vitro Assessment of the Effect of Antiepileptic Drugs on Expression and Function of ABC Transporters and Their Interactions with ABCC2. Mol Basel Switz. 2017 Sep 29;22(10).

82. Potschka H, Fedrowitz M, Löscher W. Brain access and anticonvulsant efficacy of carbamazepine, lamotrigine, and felbamate in ABCC2/MRP2-deficient TR- rats. Epilepsia. 2003 Dec;44(12):1479–86.

83. Hellman K, Aadal Nielsen P, Ek F, Olsson R. An ex Vivo Model for Evaluating Blood–Brain Barrier Permeability, Efflux, and Drug Metabolism. ACS Chem Neurosci. 2016 May 18;7(5):668–80.

84. Di Marco A, Gonzalez Paz O, Fini I, Vignone D, Cellucci A, Battista MR, et al. Application of an in Vitro Blood-Brain Barrier Model in the Selection of Experimental Drug Candidates for the Treatment of Huntington's Disease. Mol Pharm. 2019 May 6;16(5):2069–82.

85. Di Marco A, Vignone D, Gonzalez Paz O, Fini I, Battista MR, Cellucci A, et al. Establishment of an in Vitro Human Blood-Brain Barrier Model Derived from Induced Pluripotent Stem Cells and Comparison to a Porcine Cell-Based System. Cells. 2020 Apr 16;9(4).

Additional Files

Additional File 1

Additional File 1.xlsx

Data Title: Conditions and P_{eff} of 4 kD Dextran of DOE_P

Description: Contains full data set and run conditions of DOE_P that contributed to Fig. 2, Fig. 3, and Fig. 4

Additional File 2

Additional File 2.xlsx

Data Title: Conditions and P_{eff} of 4 kD Dextran of DOE_{M1}

Description: Contains full data set and run conditions of DOE_{M1} that contributed to Fig. 5

Additional File 3

Additional File 3.xlsx

Data Title: Conditions and P_{eff} of 4 kD Dextran of DOE_{M2}

Description: Contains full data set and run conditions of DOE_{M2} that contributed to Fig. 6

Figures

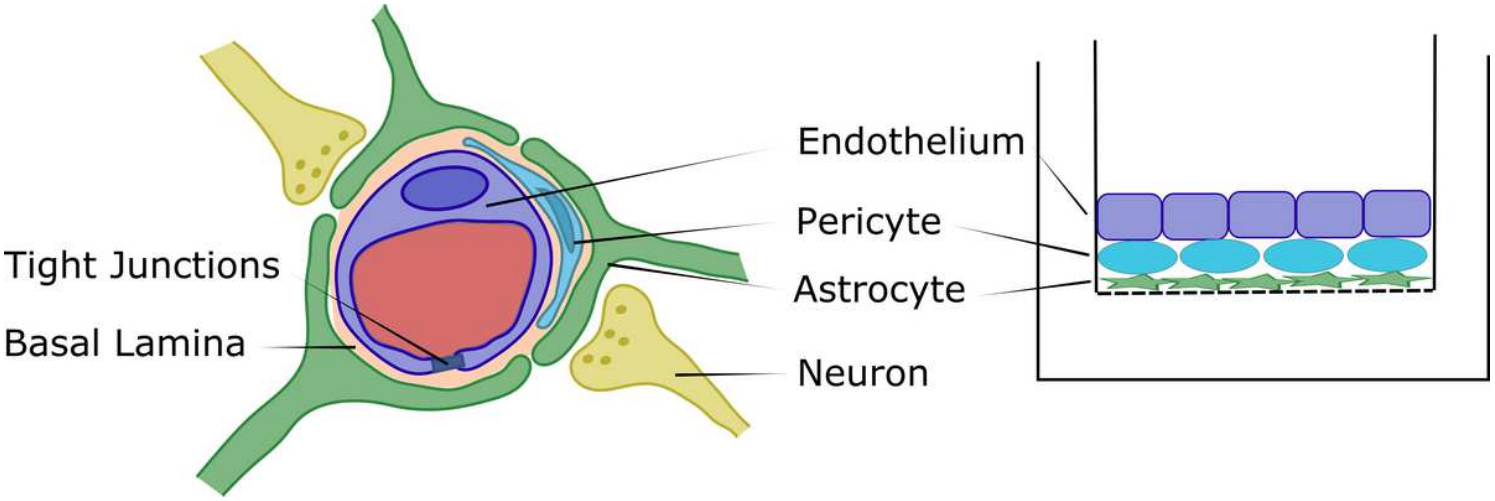

Figure 1

Cross sectional depiction of the Blood-Brain Barrier within the neurovascular unit (NVU) with the endothelium (BMECs) lining the capillary, pericytes embedded within the basal lamina, astrocytes having nearly full coverage of the BMECs and surrounding pericytes, and neurons in close contact with the astrocytes (left). The direct contact triculture model on the apical surface of a Transwell® filter support mimicking the in vivo NVU. Astrocytes are seeded first on the filter, followed by pericytes, then BMECs to generate a fully apical, direct contact triculture model (right).

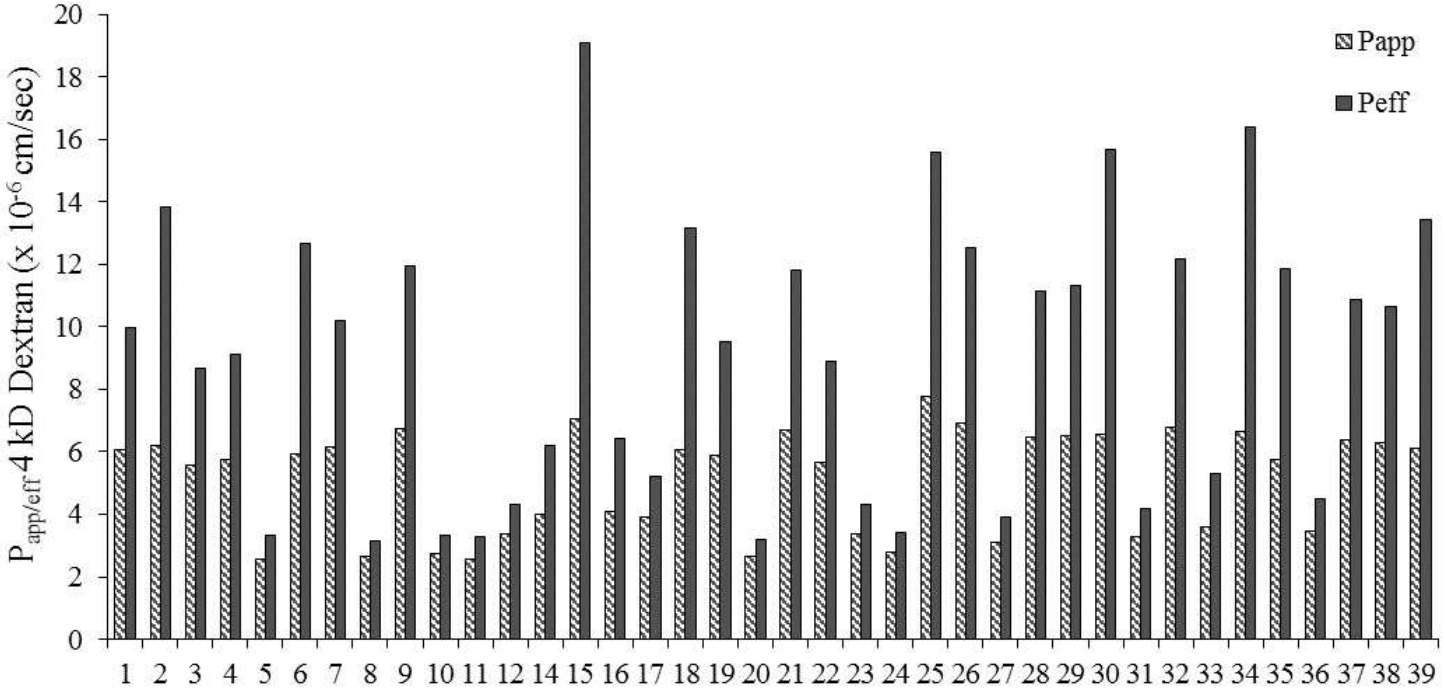

Figure 2

Papp and Peff of 4 kD FITC-Dextran across different direct contact triculture conditions of DOEP. All DOEP selected conditions were performed as n=1 for a rapid evaluation of the different parameter combinations. Condition 13 was compromised and permeability was not performed, data point was excluded from statistical analysis.

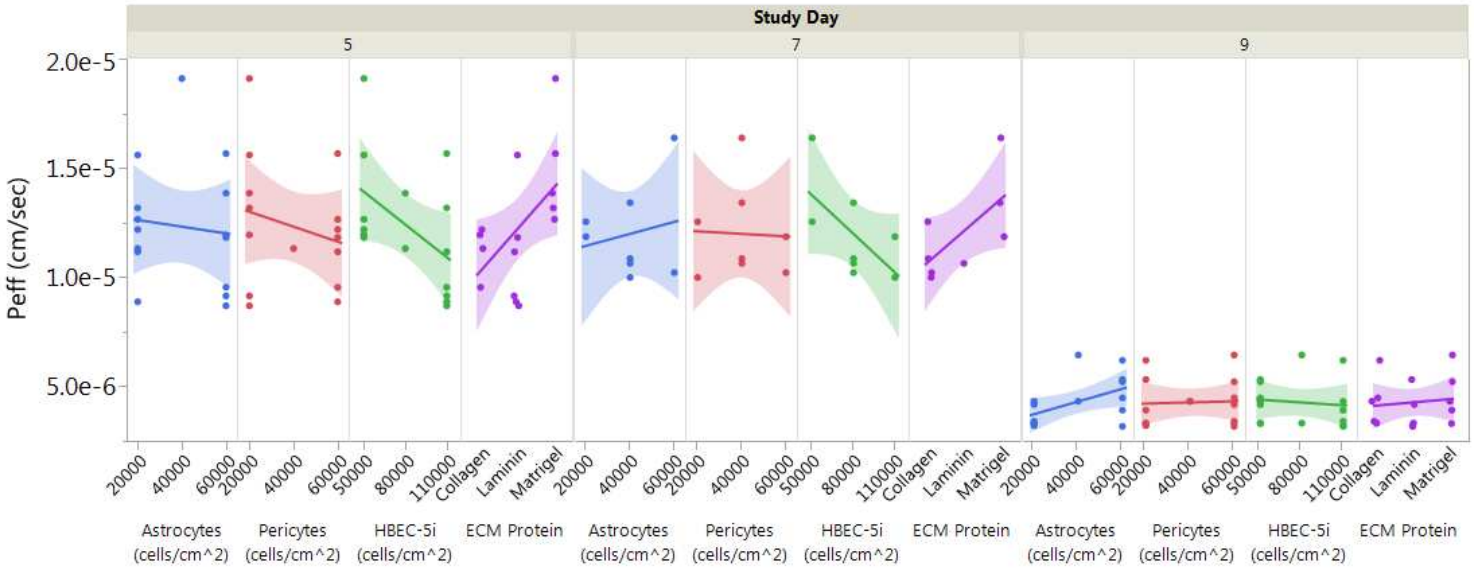

Figure 3

Peff of 4 kD FITC-Dextran for DOEP separated by factor and further by day of study showing relative trends of factor levels at increasing length of culture. All conditions are represented by single data points across the graph, n=1.

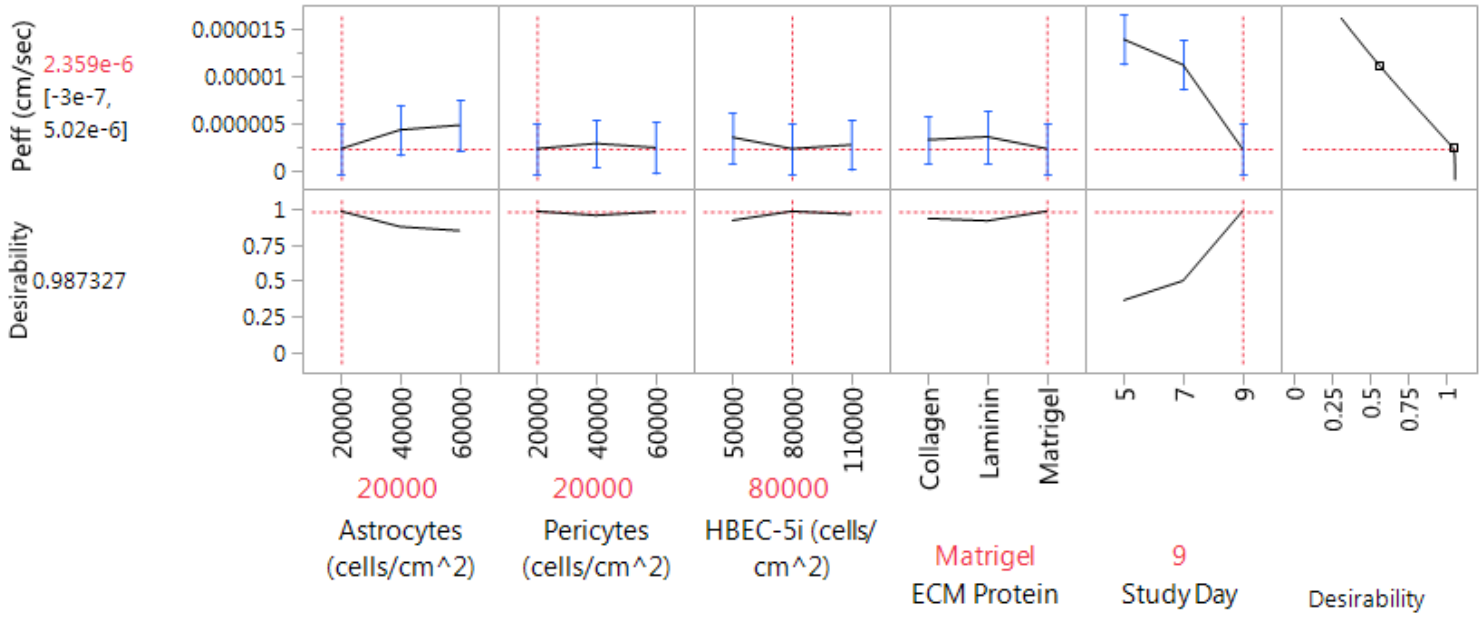

Figure 4

JMP 13.2 Prediction Profiler generated based on maximizing desirability for Peff based on DOEP. Optimal plating conditions 20,000 cells/cm2 astrocytes and pericytes, 80,000 cells/cm2 HBEC-5i, Matrigel, and 9

days of endothelial growth. Predicted Peff of 2.4 x 10-6 cm/sec for optimal conditions.

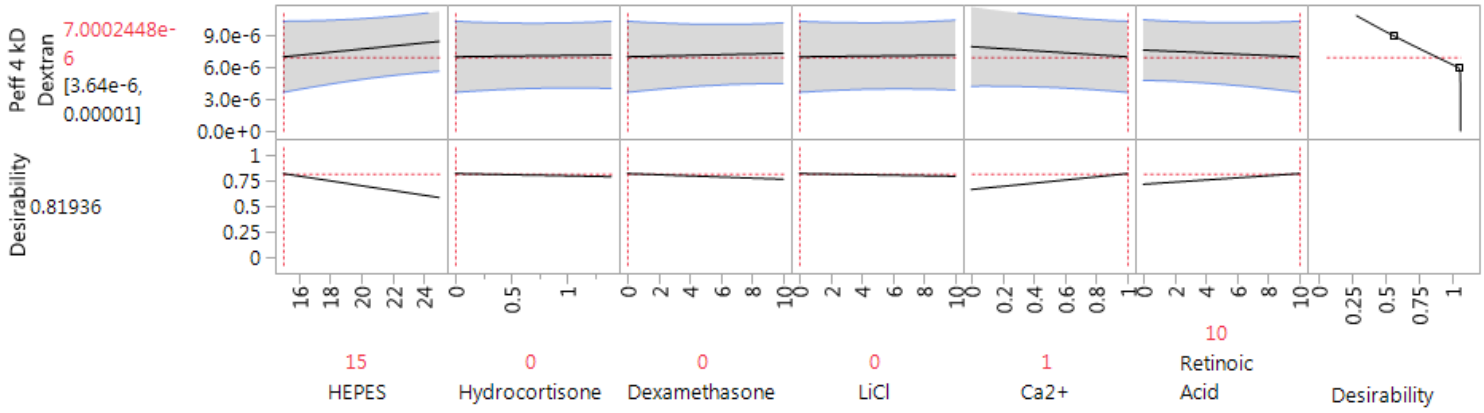

Figure 5

JMP 13.2 Prediction Profiler generated based on maximizing desirability for Peff of DOEM1. Optimal medium conditions 15 mM HEPES, 1 mM Ca2+, and 10 µM retinoic acid at 9 days of endothelial growth. Predicted Peff of 7.0 x 10-6 cm/sec for optimal conditions.

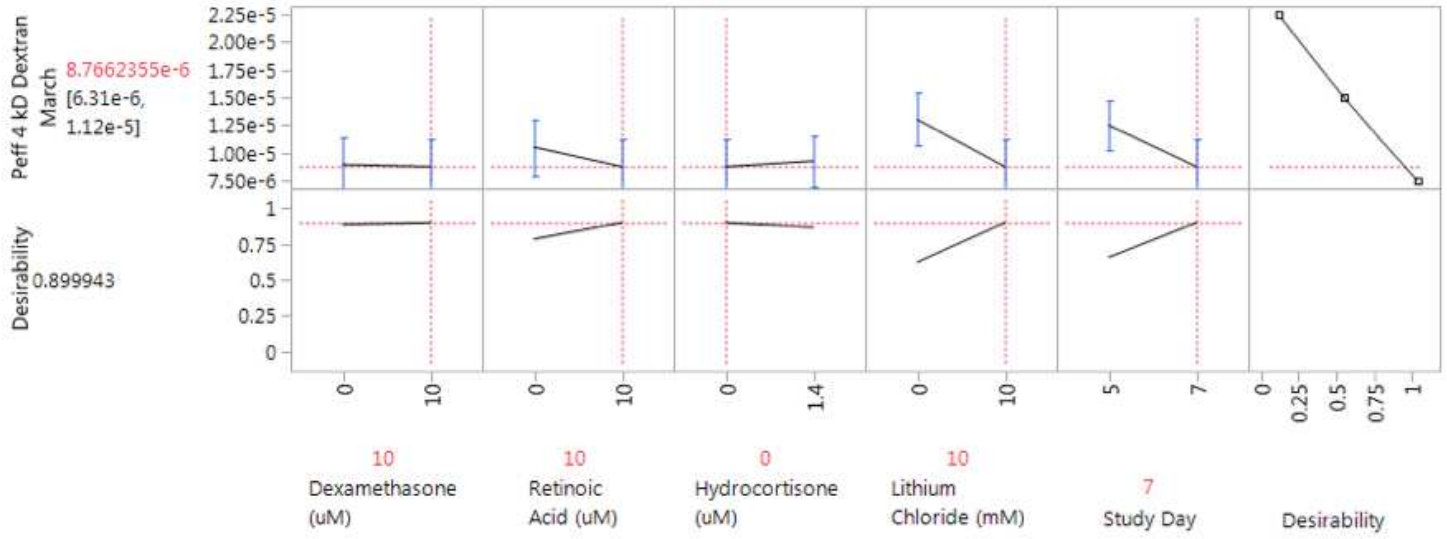

Figure 6

JMP 13.2 Prediction Profiler generated based on maximizing desirability for Peff of DOEM2. Optimal medium conditions 10 µM dexamethasone, 10 µM retinoic acid, 10 mM LiCl, through 7 days of endothelial culture. Predicted Peff of 8.8 x 10-6 cm/sec for optimal conditions.

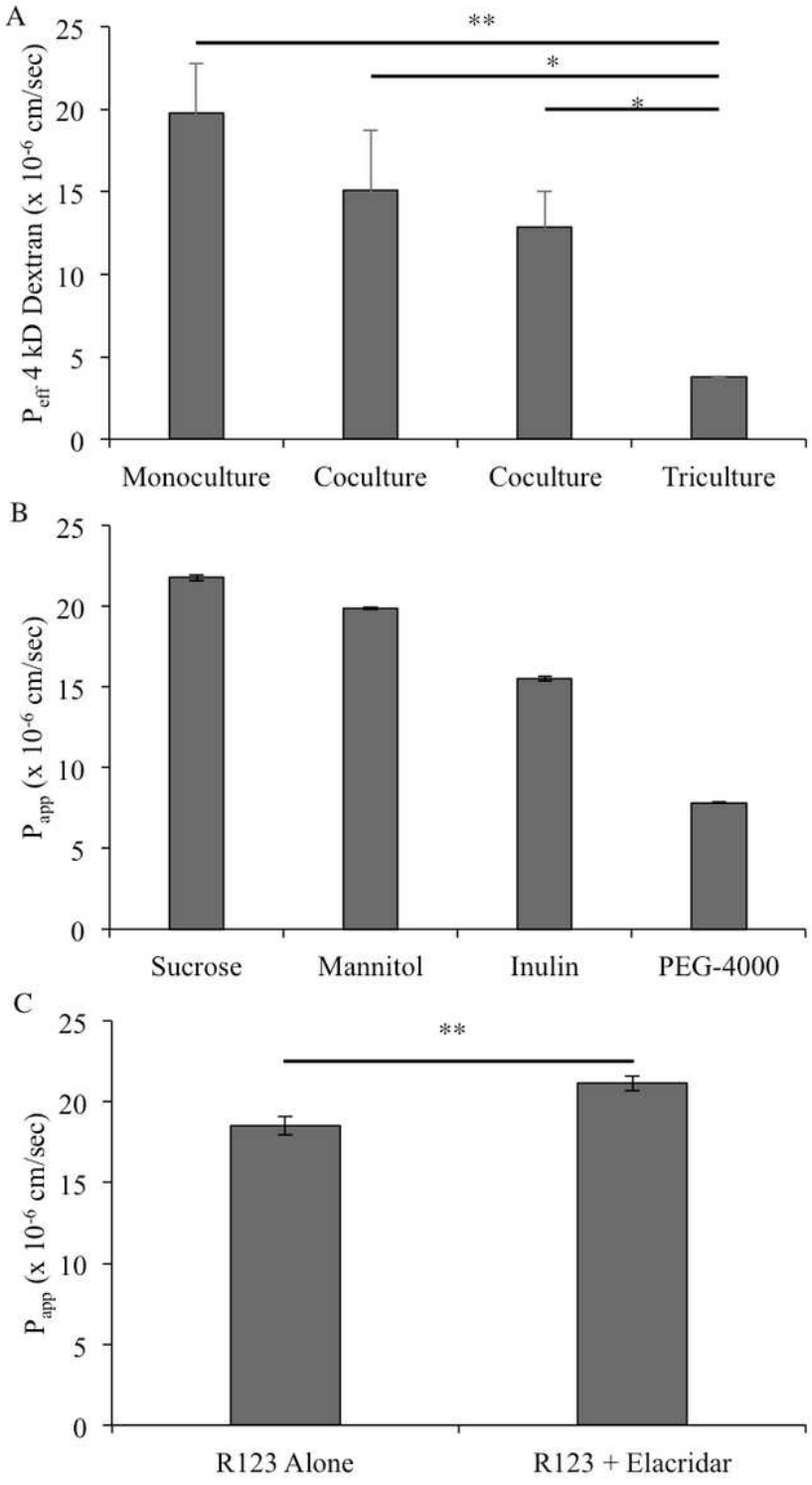

Figure 7

Optimized Triculture Permeability. (A) Effective permeability (Peff) of 4 kD FITC-dextran across an HBEC-5i monoculture, pericyte-HBEC-5i direct contact coculture, astrocyte-HBEC-5i direct contact coculture, and optimized direct contact triculture. Statistical analysis was performed with one-way ANOVA and Tukey-Kramer post-hoc test. Error bars represent one standard deviation (n=3). *, $p < 0.05$ and **, $p < 0.01$. (B) Apparent permeability of radiolabeled paracellular markers [14C]-sucrose. [14C]-mannitol, [14C]-inulin,

and [14C]-PEG-4000 across the optimized direct contact triculture. Error bars represent one standard deviation (n=3). (C) Apparent permeability of P-gp substrate rhodamine 123 (R123) in the presence and absence of P-gp inhibitor elacridar across the optimized direct contact triculture. Assays were run in triplicate and subjected to Student's t-test. Significant difference is indicated by *, $p < 0.05$ and **, $p < 0.01$. Error bars represent one standard deviation (n=3).

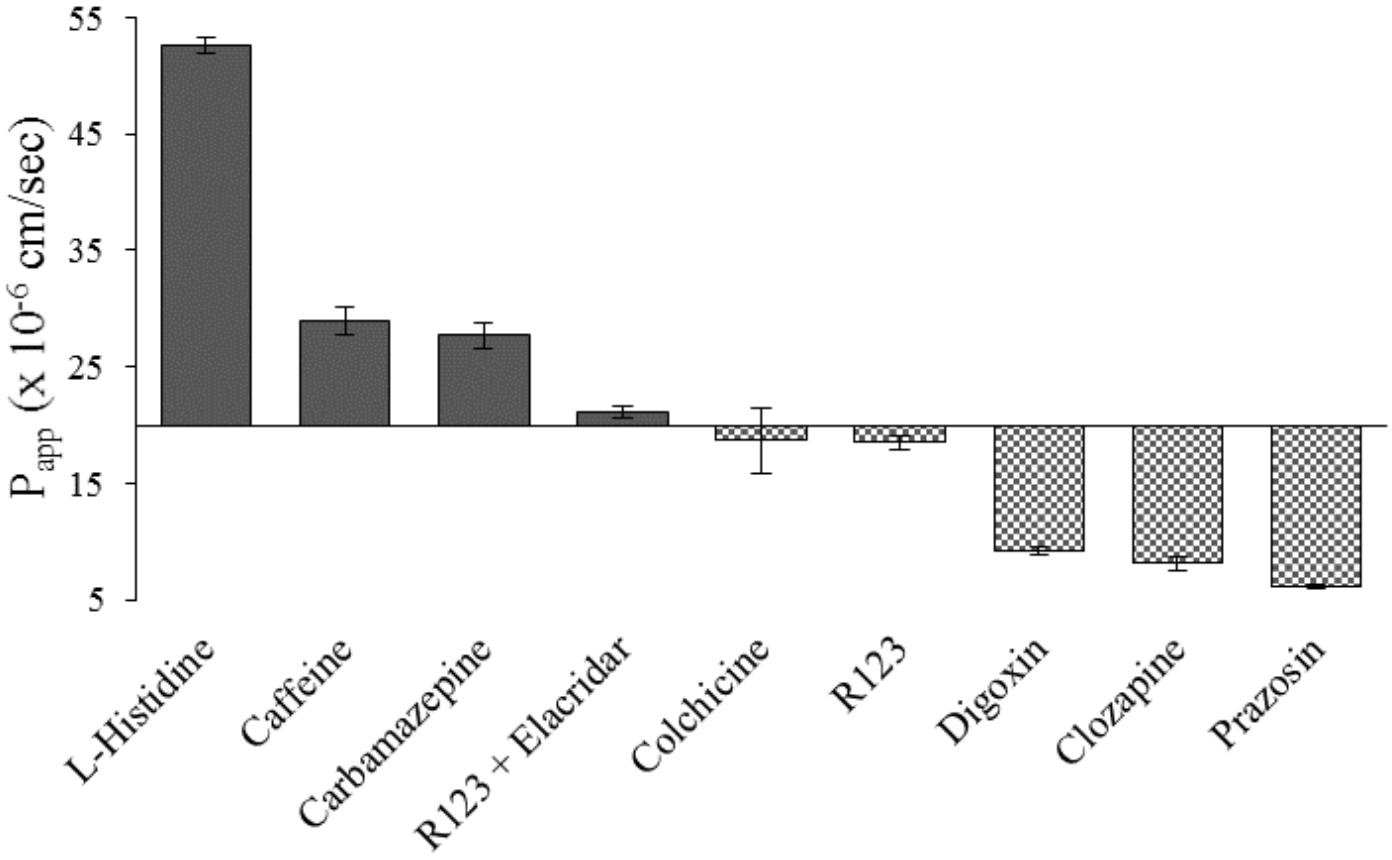

Figure 8

Apparent permeability of BBB positive (L-histidine, carbamazepine, and rhodamine 123 in the presence of P-gp inhibitor elacridar) and negative (colchicine, rhodamine 123, digoxin, clozapine, and prazosin) permeants across the optimized direct contact triculture. Assays were performed in triplicate. Error bars represent one standard deviation (n=3).

Supplementary Files

This is a list of supplementary files associated with this preprint. Click to download.

- AdditionalFile1.xlsx
- AdditionalFile2.xlsx
- AdditionalFile3.xlsx